Aus der

Universitätsklinik für Zahn-, Mund- und Kieferheilkunde

Tübingen

Abteilung Klinik und Poliklinik für Mund-, Kiefer- und Gesichtschirurgie

Analysis of the Phenotypic Effects of 2D- and 3D-Cultured Jaw Periosteal Cells on THP-1-Derived Macrophages

Inaugural-Dissertation

zur Erlangung des Doktorgrades

der Zahnheilkunde

der Medizinischen Fakultät

der Eberhard Karls Universität

zu Tübingen

vorgelegt von

He, Fang

2022

Dekan: Professor Dr. B. Pichler

1. Berichterstatter: Professorin Dr. D. Alexander-Friedrich
2. Berichterstatter: Privatdozentin Dr. S. Ehnert

Tag der Disputation: 05.08.2022

Contents

List of figures

List of tables

List of abbreviations

2D: two-dimension

3D: three-dimension

BTE: bone tissue engineering

β-TCP: β-tricalcium phosphate

CD-: cluster of differentiation-

CCL-: chemokine (C-C motif) ligand-

CXCL-: chemokine (C-X-C motif) ligand-

DAMPs: damage-associated molecular patterns

G-CSF: granulocyte-colony stimulating factor

THP-1: human monocytic cell line

HSCs: Hematopoietic stem cells

IFN-γ: interferon-γ

IL- : interleukin-

JPCs: jaw periosteal cells

LPS: lipopolysaccharide

M0: immature macrophages

M1: classically activated macrophages

M2: alternatively activated macrophages

MSCs: mesenchymal stem cells

OB: osteogenically induced differentiation

PAMPs: pathogen-associated molecular patterns

PCR: polymerase chain reaction

PMA: phorbol 12-myristate 13-acetate

PRRs: pattern recognition receptors

SDF-1: stromal cell-derived factor 1

TLRs: toll-like receptors

TNF-α：tumor necrosis factor-alpha

1. Introduction

1.1. Stem cell and bone tissue engineering

1.1.1. Bone tissue engineering and stem cell source

Tissue engineering is a field creating natural alternatives to regenerate defective tissues and organs due to injury, disease and development defects that have failed to heal by themselves [1]. In critical-size bone defects, bone tissue engineering (BTE) provides a challenging but ideal treatment strategy for bone regenerative medicine [2]. The aim of BTE is to create functional bone regeneration through a combination of cells, biomaterial scaffolds and tissue-inducing factors [3]. In general, the following processes are involved in cell-based BTE [4, 5]: First, autologous or allogeneic cells are primarily cultured and expanded in vitro to obtain sufficient cells for clinical applications. In the next step, the expanded cells are induced to osteogenic/chondrogenic differentiation and seeded onto three-dimensional (3D) biomaterials with or without growth factors. Subsequently, the prepared constructs can be cultured in vitro in a bioreactor system until the maturation stage or implanted directly into the recipient in vivo for further development. The ultimate goal is to create a functional tissue that will fit with the defective site for the purpose of bone/organ regeneration [4]. Figure 1 shows a schematic paradigm of the bone tissue engineering procedure.

In terms of material design and selection for BTE purposes, understanding and mimicking the composition and structure of native bone tissue and the selection of appropriate biomimetic natural biomaterials can enhance the success rate of BTE [6, 7]. β-tricalcium phosphate (β-TCP), characterized as osteoconductive, osteoinductive and cell-resorptive, is a widely used and adequate synthetic bone graft substitute [8].

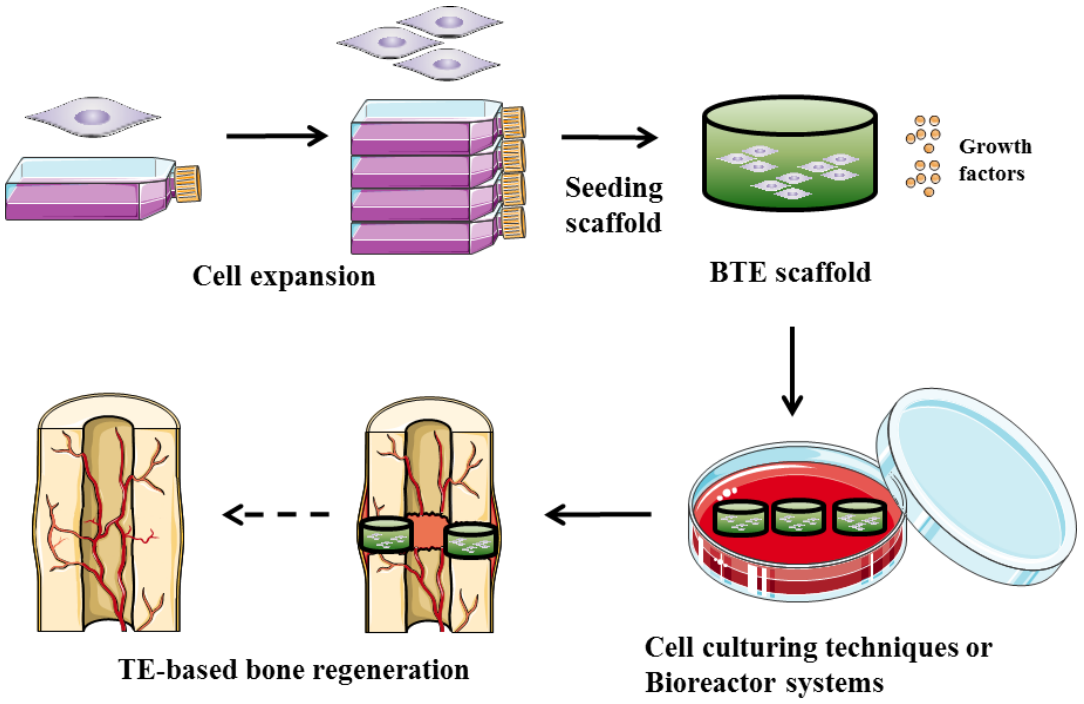

Figure 1. A schematic paradigm of bone tissue engineering [4, 5]. To obtain sufficient cells for clinical applications, autologous or allogeneic cells are first cultured and expanded in vitro. Next, the expanded cells are differentiated into the osteogenic/chondrogenic lineage and seeded on 3D biomaterials with or without growth factors. After preparation, the constructs can be cultured in vitro in a bioreactor system until maturity or implanted directly into a recipient in vivo for further development. For bone/organ regeneration, functional tissue must be created at the defective site.

In the BTE approach, cells are one of the primary determinants of success since they are the basic functional unit of the organism [9]. Currently, several types of differentiated cells (e.g. osteoblasts) and undifferentiated cells (e.g. embryonic stem cells, adult stem cells from a variety of tissues, perinatal stem cells and induced pluripotent stem cells) have been applied alone or in combination with various biological scaffolds for bone restoration [10]. Differentiated cells (e.g. osteoblasts) have a limited proliferative lifespan. In contrast, stem cells that sit at

the apex of the differentiation hierarchy can self-renew and develop into highly specialized cells, making them more suitable for tissue engineering and regenerative purposes [11]. Considering their availability, ethical issues, tumorigenicity and immune tolerance properties of various stem cell subtypes, mesenchymal stem cells (MSCs) are comprehensively considered as the best source of stem cells for BTE at present (Table 1) [10, 12, 13].

Table 1. Comparison of cell sources used in BTE [10, 12, 13].

Cell type	Accessibility	Ethical issue	Tumorigenicity	Immune tolerance
Autologous osteoblasts	difficult	no	no	no
Embryonic stem cells	difficult	yes	yes	no
Induced pluripotent stem cells	difficult	no	yes	partly
Mesenchymal stem cells	easy	no	no	yes

1.1.2. Mesenchymal stem cells

Mesenchymal stem cells (MSCs) are multipotent stromal/stem cells that possess self-renewal ability and tri-lineage differentiation potential and show extreme plasticity [14, 15]. The International Society for Cellular Therapy (ISCT) set minimal standards for defining MSCs [16]: 1) MSCs are defined as plastic

adhesion cells and fibroblast-like shapes under conventional culture conditions. 2) In vitro, MSCs can differentiate into osteogenic, adipogenic, or chondrogenic cells. 3) The cultured MSCs express CD73, CD90 and CD105 on their surfaces, while they do not express CD11b, CD14, CD19, CD34, CD45, or HLA-DR (Figure 2). In addition, the immunomodulatory ability and immune escape properties of MSCs make them more suitable for the BTE approach when allogeneic-derived cells are used, and some of them have already entered the phase I and I/II stage of clinical trials [17-19]. MSCs acting as sensors and switchers of inflammation can be classified into pro-inflammatory (MSC-1) and anti-inflammatory (MSC-2) phenotypes (Figure 2) [20]. Under different microenvironments (such as different levels of TNF-α/IFN-γ stimulation), MSCs can orchestrate innate or adaptive immune responses by releasing a series of heterogeneous mediators, including cytokines, chemokines, exosomes and various immunosuppressive metabolites [19, 21]. Vice versa, the immune microenvironment reshaped by the mediators also feeds back to influence the biological property of MSCs themselves, such as osteogenic differentiation [22, 23]. When implanting biological scaffolds into a recipient for BTE purposes, both local/mobilized endogenous MSCs and transplanted exogenous MSCs will communicate with local immune cells in a complex pattern [24-26]. Currently, the homeostasis of inflammatory microenvironments is the main challenge for the efficacy of BTE constructs, but MSCs may offer a viable solution for inflammation regression and tissue homeostasis at the site of bone defects [27, 28].

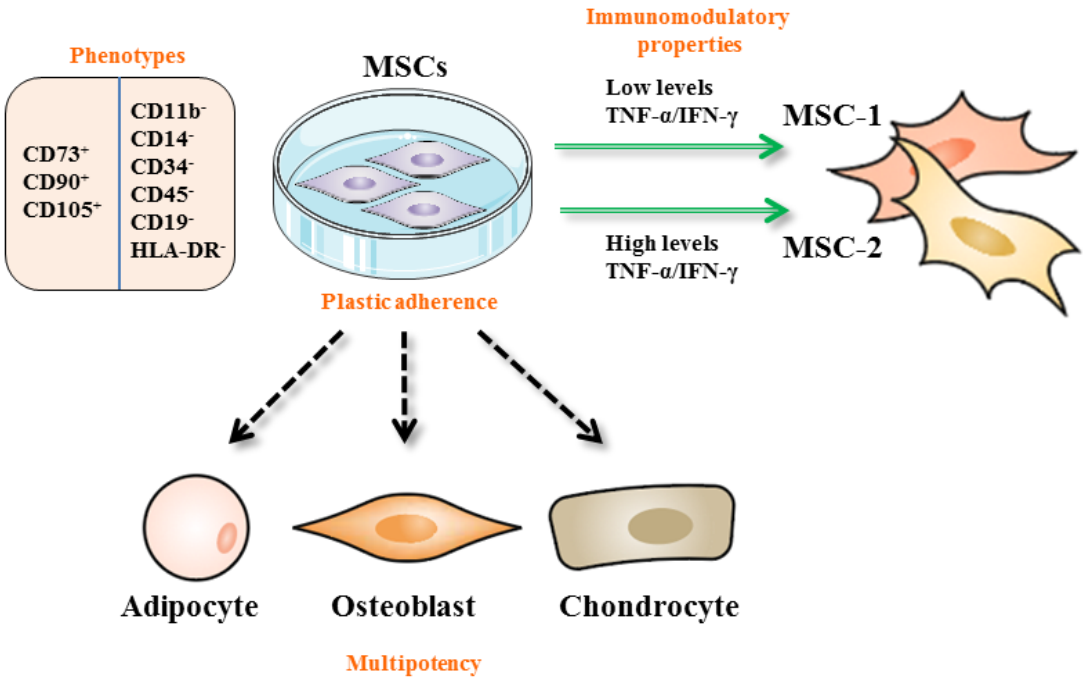

Figure 2. The characteristics and immunomodulatory properties of MSCs [16, 20, 29]. MSCs exhibit a specific phenotype, fibroblast morphology and multipotency. The intensity and complexity of inflammatory stimuli dictate the plasticity of MSC immune regulation. MSCs exhibit an immunosuppressive phenotype (MSC2) in high levels of TNF-α/IFN-γ environment. The low levels of TNF-α/IFN-γ may allow MSCs to exhibit a pro-inflammatory phenotype (MSC1).

1.1.3. Jaw periosteum-derived mesenchymal stem cells

MSCs derived from bone marrow, adipose tissue, tooth tissue and periosteum tissue represent popular cell candidates for the study of regenerative medicine and tissue engineering [30]. However, different in situ derived MSCs do not have the same level of multipotency [11]. The periosteum is the membrane that attaches to the outer surface of all bones except the long bony joints, and it consists of dense irregular connective tissue, which can be divided into an external "fibrous layer" and an internal "cambium layer" [31]. One of its characteristics is mechanoreception. This means that mechanical loading can modify the phenotype of periosteal progenitor cells and induce periosteal-based

bone repair and regeneration [32-34]. Compared with MSCs harvested from other tissues, the periosteum-derived MSCs show stronger osteogenic/chondrogenic potential and are considered an excellent cell source for bone regeneration applications [35-38]. The periosteal cells derived from the jaw tissue (jaw periosteal cells, JPCs) show under high mechanical loading, superior osteogenic properties and immunosuppressive effects on dendritic cells, which have been demonstrated in the previous studies of our group [37, 39-42].

Undoubtedly, the success of BTE constructs is closely related to the immunomodulatory properties of osteogenically differentiated JPCs. Macrophages are the most critical myeloid cells that play multifunctional roles during the innate and adaptive immune reactions [43, 44]. Osteal macrophages are closely related to osteoblasts and can synergistically support bone formation, as well as being regulators of osseous wound healing [45]. These cells are abundantly present when BTE constructs are implanted into the defect site, and they represent the primary immune cell population to respond to foreign pathogens and materials [46, 47]. Therefore, understanding macrophage regulation/modulation by JPCs is essential to ensure the success of JPC-colonialized BTE constructs.

1.2. Macrophages

1.2.1. Macrophage origin and function

Macrophages can be recruited into organ tissues from the mononuclear phagocytic system or independently originate from embryonic progenitors [48] (Figure 3). The haematopoietic stem cells (HSCs) within the bone marrow develop into immature monocytes, which are strategically stored in the specific reservoir spleen or migrate along with the circulation [49]. Monocytes extravasate through the endothelium to differentiate into macrophages located in the infected

or injured tissue after subsequent activation to heterogeneous macrophage subtypes in response to stimulation [49, 50]. Additionally, tissue-resident macrophages from the yolk sac or fetal liver precursors during fetal development also function as sentinel cells against the microbes and maintain tissue homeostasis [51].

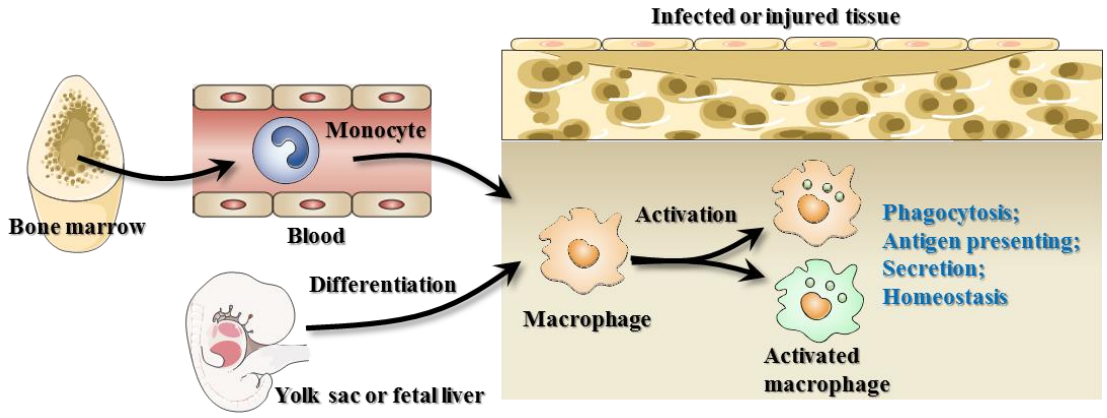

Figure 3. The origins, recruitment into infected or injured tissues and functions of macrophages [48, 52-54]. Macrophages derive from phagocytic mononuclear cells or from embryonic progenitors. The functions of macrophages involve phagocytosis, antigen-presenting, secretion and homeostasis.

As a type of "professional" phagocytic cells, the macrophages are characterized by phagocytosis and initiation of an immune response [52] (Figure 3). They have the ability to engulf and digest cellular waste, foreign substances, bacteria, and cancer cells, as well as anything else that lacks the proteins found on the surface of healthy body cells [52]. Whether it is ingesting pathogens or efferocytosis to apoptotic cells, the primary role of this phagocytosis process is to protect the host from different types of infection or injury [55, 56].

Another essential role of macrophages is their antigen-presenting functions in

adaptive immunity [53] (Figure 3). The phagocytosis and antigen presentation of macrophages are not independent but closely interwoven [52-54]. After digesting pathogens, a macrophage can present the pathogen's antigen to the corresponding T helper cell, and multiple receptor-ligand interactions carefully orchestrate this process [54]. When pattern recognition receptors (PRRs), including Toll-like receptors (TLRs), C-type lectin receptors, scavenger receptors, retinoic acid-inducible gene 1-like helicase receptors and NOD-like receptors, on macrophages were activated by pathogen-associated molecular patterns (PAMPS) from microbes or damage-associated molecular patterns (DAMPs) from cell damage or death, macrophages can internalize substances and form phagosomes [49, 57]. After the phagosome fuses with cytoplasmic lysosomes forming phagolysosomes, the microbes or cell debris in the phagolysosome are killed or digested [58]. Under the influence of hydrolases, pathogen-derived peptides can be generated and presented to T helper cells via MHC class II molecules [58]. Then the antigen-specific T cells may be further activated by the assistance of co-stimulation signals (CD80/CD86 on macrophages) [59].

Macrophages can also recruit monocytes/leukocytes from the blood to migrate into injured sites to initiate or enhance the protective response to infections [54]. This process is mediated by its cytokines/chemokines secretion or the factors released from its pyroptosis [54] (Figure 3).

Besides, macrophages can stimulate new blood vessel growth and synthesize collagen-rich extracellular matrix to improve the repair of injured tissues [54].

1.2.2. Macrophage polarization

Macrophages are extremely heterogeneous cells that exhibit fast phenotypic change in response to microenvironmental inputs [60]. Although distinct subpopulations of macrophages have been reported, it is widely accepted that

macrophages constitute a spectrum of functional phenotypes/characteristics rather than discrete fixed subtypes [49]. Nowadays, diverse macrophage subpopulations with different immunological functions have been identified. In general, M1 macrophages (classically activated macrophages) mediate host defence against various microorganisms and also mediate anti-tumour immune responses whilst promoting Th1 responses [60, 61]. Another phenotype of M2 macrophages (alternatively activated macrophages) elicits anti-inflammatory functions and regulates wound healing while supporting Th2-associated effector functions [61]. Based on distinct gene expression profiles caused by different microenvironment exposure, M2 macrophages can be further divided into M2a, M2b, M2c and M2d subsets [62, 63]. This variety of phenotypes in vivo needs to be considered for in vitro research. THP-1, a monocytic cell line generated from human leukemia, is the most frequently utilized cell line for in vitro research of primary human macrophage activity [64, 65]. This is because suspension THP-1 cells exhibit the morphological and functional properties of human M0 macrophages upon stimulation with phorbol 12-myristate 13-acetate (PMA) [65] (Figure 4). By using lipopolysaccharide (LPS) and interferon-γ (IFN-γ), M0 macrophages polarize into classically activated M1 macrophages; In contrast, M2 macrophage activation can be induced by interleukin-4 and interleukin-13 [66] (Figure 4).

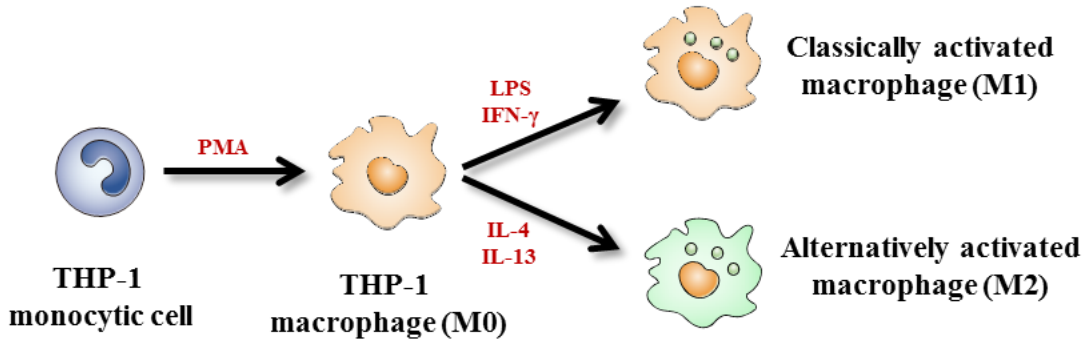

Figure 4. THP-1 derived macrophage polarization in in vitro studies. THP-1 monocytic cells acquire human M0 macrophage phenotypes under PMA stimulation. With lipopolysaccharide (LPS) and interferon-γ (IFN-γ), M0 macrophages polarize into classically activated M1 macrophages. By contrast, interleukin-4 (IL-4) and interleukin-13 (IL-13) may activate M2 macrophages.

1.3. Coculture systems

Cell coculture is an effective method to investigate the dynamic crosstalk between different types of cells [67, 68]. Cellular contacts can be directly involved in intercellular stimulation to affect cellular metabolism. However, the direct contact coculture model cannot identify whether the effects comes from secreted factors or not [69]. In contrast, non-contact interactions between cells (such as the secretion of hormones, cytokines, chemokines, exosomes) can not only mutually regulate cellular metabolism but also play a vital role in the regulation of cell motility (such as immune cell migration and stem cell homing), which is the effective way to investigate the paracrine cell interaction [68, 70].

The indirect coculture method of transferring conditioned medium/supernatant/secretome from the donor cells to the target cells has some limitations. For example, the continuous interaction between cells and the feedback of target cells to donor cells cannot be monitored. The traditional "transwell coculture" or "vertical type" culture system effectively addresses this limitation. However, the filter is clogged by cells, the different medium volume in the two chambers and the difficult cell observation in the upper chamber are challenges in this coculture system. The innovative horizontal coculture system provides a good solution for the above-mentioned disadvantages by connecting two identical chambers laterally [69]. The horizontal coculture system (UniWells^{TM}) has the following advantages (Figure 5): 1) microscopy can visualise the cells in both chambers simultaneously. 2) The filter does not get clogged with cells. 3)

Cells are cultured on the same bottom material and using the same volume of culture medium. 4) The two chambers can be combined or used separately. Therefore, the horizontal coculture system may provide effective signal communications for the coculture between two cell types as described in the following works between JPCs and macrophages.

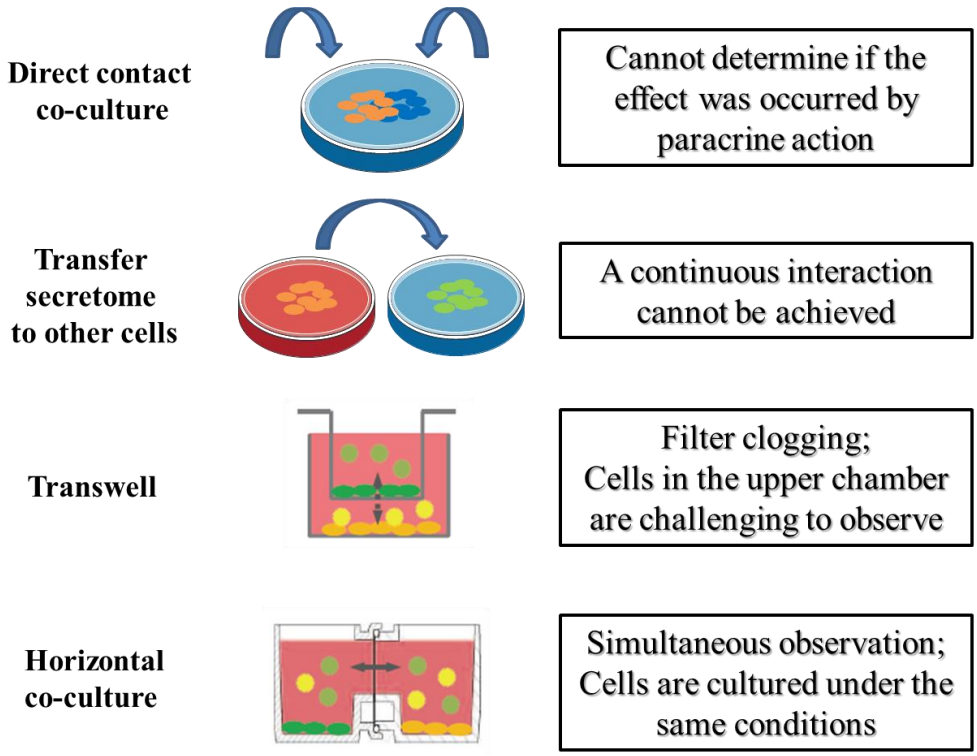

Figure 5. Comparison of different coculture systems (image refer to ICCP/UniWells™). The different coculture models, such as the contact coculture, the transfer secretome method, the transwell system and the horizontal coculture plate, have unique characteristics.

1.4. Aims of the present dissertation

JPCs show MSCs characteristics and may possess similar immunoregulative abilities, representing a promising cell source for BTE [41, 42, 71-74].

Macrophages play a central role in innate immunity, and their alternative activation can facilitate wound healing and tissue repair, which may contribute to the application of BTE constructs [75]. Our previous studies demonstrated that 2D-cultured JPCs and JPCs colonialized β-TCP scaffolds (3D cultured JPCs) could suppress DC maturation in an indirect transwell coculture system [41, 76]. In this study, we try to investigate the effects of JPCs on THP-1 macrophage phenotypic polarization under a direct contact or indirect coculture model [71, 72]. Furthermore, to investigate the paracrine secretion effects of JPCs on M1/M2 macrophage polarization, an innovative horizontal coculture system was applied to coculture JPCs and THP-1-derived M1/M2 macrophages [72]. The soluble factors secreted from JPCs or macrophages in the coculture system were also analyzed. These factors may explain the potential paracrine mechanism of JPCs acting on macrophages polarization.

In addition, the three-dimensional (3D) cultures can mimic the biochemical and biophysical properties of the native 3D microenvironment by incorporating specific biomaterials [77]. β-tricalcium phosphate (β-TCP), one of the promising bone graft substitutes used for BTE [8], was utilized to develop 3D-cultured JPC-based constructs in the present study. The effects of both 2D-cultured JPCs and JPCs colonialized β-TCP scaffolds on macrophages polarization were investigated and included in this thesis.

Furthermore, since JPCs possess multipotency, their osteogenically induced differentiation should be pre-defined before transplantation into the bone defect sites for BTE approaches [72]. So, the interactions between osteogenically generated JPCs and macrophages were examined concurrently.

Based on the findings of this work, elucidating the paracrine secretion effects of 2D- and 3D-cultured JPCs to THP-1 macrophages polarization may contribute to the future use of JPCs in BTE approaches.

2. Materials and Methods

2.1. The main materials used in the experiment

Table 2. The mediums, reagents and kits used in the experiment.

Medium/Reagent/Kit	Company
RPMI 1640 medium	Thermo Fisher Scientific
DMEM/F12 medium	Thermo Fisher Scientific
FBS	Sigma-Aldrich
Penicillin/streptomycin	Lonza
Amphotericin B	Biochrom AG
2-mercaptoethanol	Sigma-Aldrich
TrypLE-Express	Thermo Fisher Scientific
PMA	Sigma-Aldrich
Vitronectin	Gibco
LPS	Sigma-Aldrich
IFN-γ	Sigma-Aldrich
IL-4	Sigma-Aldrich
IL-13	Sigma-Aldrich
β-TCP scaffolds	Curasan AG
L-ascorbic acid	Sigma-Aldrich
β-glycerophosphate	PanReac AppliChem
NucleoSpin RNA kit	Macherey-Nagel
SuperScript VILO Kit	Thermo Fisher Scientific
DNA master SYBR Green I kit	Roche
LunaScript® RT SuperMix Kit	New England Biolabs
Luna® Universal Probe qPCR Master Mix	New England Biolabs
Human cytokine proteome profiler array kits	R&D Systems

Table 3. The main laboratory equipment/instruments used in the experiment.

Main laboratory equipment/instrument	Company

Guava EasyCyte 6HT-2L flow cytometer	Merck Millipore
NanoDrop One instrument	Thermo Fisher Scientific
Real-time LightCycler System	Roche
QuantStudio 3 Real-Time PCR Instrument	Thermo Fisher Scientific

2.2. In vitro cell culturing of THP-1 cells and JPCs

"THP-1 cells (from the ATCC) were grown in RPMI 1640 medium. As a supplement for THP-1 cell expansion, we used 10% heat-inactivated FBS, 1% penicillin/streptomycin, 1% amphotericin B and 0.05 nM 2-mercaptoethanol." [72]

"After receiving clearance from the local ethics committee (No. 618/2017BO2), JPCs from three donors were included in the research. We cultivated and expanded JPCs in DMEM/F12 medium containing 5% hPL (provided by the Institute for Clinical and Experimental Transfusion Medicine of the University Hospital Tübingen), 1% penicillin/streptomycin and 1% amphotericin B. TrypLE-Express was used for JPCs passaging." [72]

"JPCs or THP-1 cells were cultured and expanded in flasks of 25 or 75 cm^2 at 37 °C in a 5% CO_2 incubator. Every two days, the culture medium was replaced." [72]

2.3. Contact coculture of JPCs and THP-1 macrophages (This section published in "He et al., International journal of molecular sciences, 2021, 22(9): 4310")

The directly mixed coculture of JPCs and macrophages was conducted for cell contact coculture.

"Prior to coculture, JPCs (2×10^4/well) were grown under 5 % hPL DMEM/F12 in 24-well plates for 48 hours. Meanwhile, THP-1 cells (4×10^5/well) were induced to

differentiate into M0 macrophages in separate 24-well plates. A 5% hPL RPMI1640 medium containing 5 nM PMA was used for M0 macrophage differentiation for 48 hours." [71]

"For the direct contact coculture, JPCs were removed from the 24-well plate using TrypLE-Express and resuspended in 5% hPL RPMI 1640 medium with 15 ng/mL LPS and 20 ng/mL IFN-γ (for M1 coculture) or with 20 ng/mL IL-13 and 20 ng/mL IL-4 (for M2 coculture). Following that, seeding of the JPC suspension into M0 macrophages was performed (M1/M2-JPC groups). The M1/M2 macrophages monoculture control group (M1/M2-Control groups) received cell-free 5% hPL RPMI 1640 medium supplemented with LPS/IFN-γ or IL-4/IL-13." [71]

"Following 5 days of mixed contact coculture with JPCs and M1 or M2 macrophages, macrophages were phenotypically examined using flow cytometry to evaluate their polarization state. The macrophage-specific marker CD68 was utilized to identify THP-1 macrophages in the above direct coculture systems. The M1 or M2 polarization was determined using CD80 (M1 macrophage surface marker) or CD206/CD163 (M2 macrophage surface markers). Figure 6 shows the procedure of the direct coculture experiment." [71]

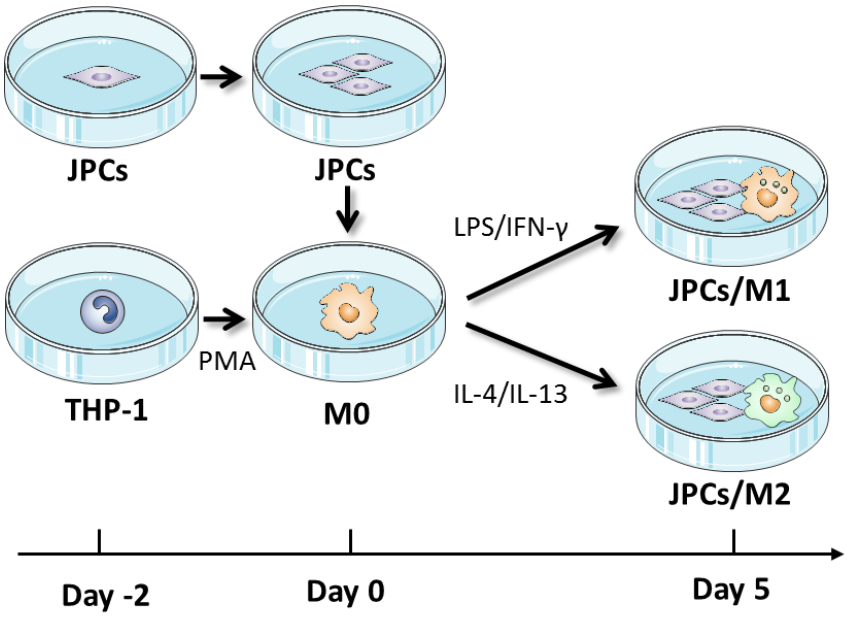

Figure 6. The experimental approach for the contact coculture of JPCs and macrophages [71].

2.4. Horizontal coculture of 2D- and 3D-cultured JPCs and THP-1 macrophages

2.4.1. Horizontal coculture system

“Ginreilab Inc. (Uchinada, Japan) provided the horizontal coculture plates (also named UniWells^{TM}) with 0.6 μm filters and the 96-well plate-size adaptor. A coculture plate comprises the components listed below: chamber A, chamber B, a cover, a common cover, an O-ring, and an adapter. Figure 7 illustrates the construction of the horizontal coculture plate.” [72]

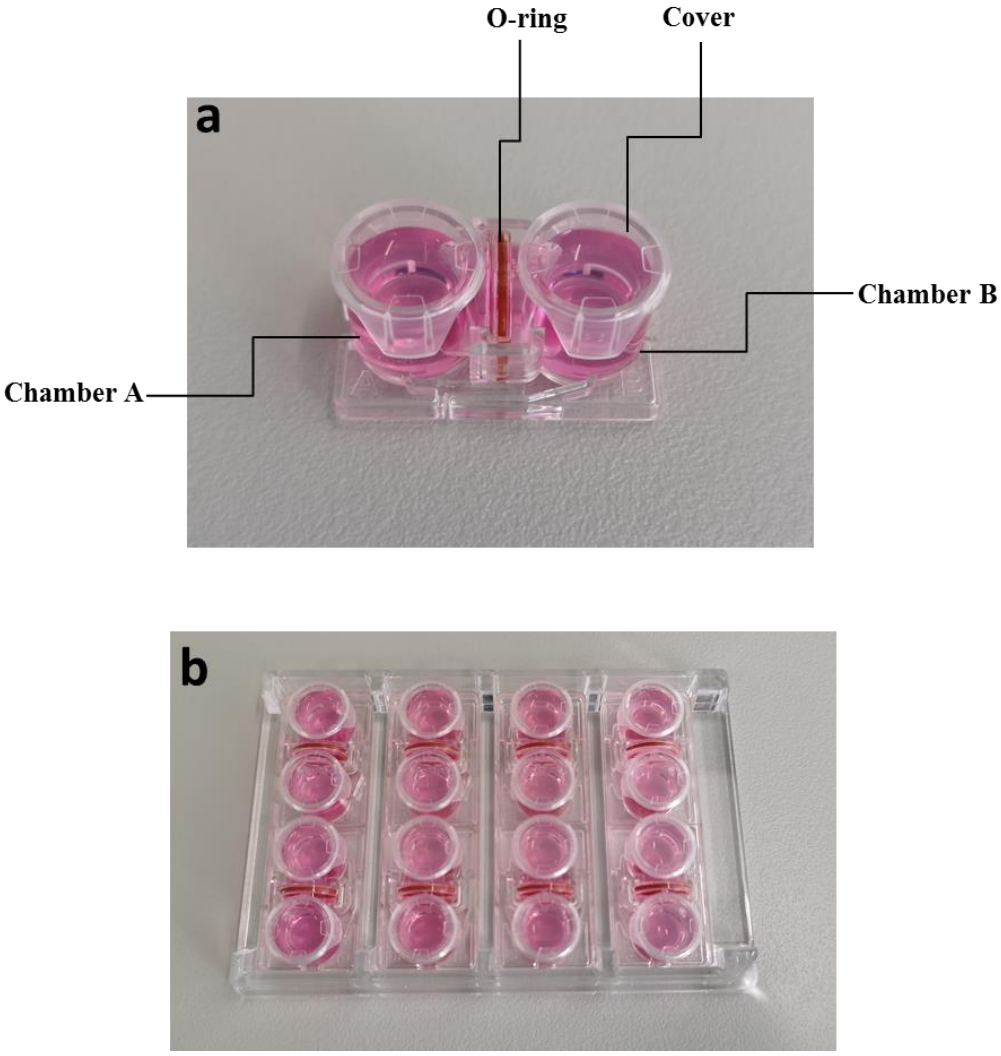

Figure 7. Images of the horizontal coculture system. (a): The structure of an assembled coculture plate. (b): The horizontal coculture plates were set into a 96-well plate-size adapter.

2.4.2. **Horizontal coculture of 2D-cultured JPCs and macrophages** (This section published in “He et al., Biomedicines 2021, 9(12), 1753”)

“Prior to initiating the horizontal coculture, a single culture of JPCs or THP-1 macrophages was conducted by assembling the chamber A/chamber B, the cover, and the common cover.” [72]

“In preparation for the JPCs preculture on day 0, passage 3 of JPCs (2×10^4 cells/chamber) were resuspended in a 1.5 ml volume of 10% hPL DMEM/F12 medium. And the cell suspension was seeded into a vitronectin-precoated chamber A. After 48 hours of growth, JPCs were cultivated for five days in the separate chambers under untreated conditions (DMEM: 10% hPL DMEM/F12) or osteogenic conditions (OBDMEM: 10% hPL DMEM/F12 + 100 mM L-ascorbic acid + 10 mM β-glycerophosphate). Every other day, the medium was changed. For the medium control groups, 1.5 mL of JPCs-free medium (10% hPL DMEM/F12 with or without osteogenic stimuli) was introduced to a parallel vitronectin-precoated chamber following the identical medium change protocols. In Table 4, we define the abbreviations used.” [72]

Table 4. Used abbreviations for 2D-cultured JPCs/OBJPCs in the coculture groups [72]. (Table published in “He et al., Biomedicines 2021, 9(12), 1753”)

Abbreviation	Group	Cells	Added reagents
DMEM	medium control	-	-
OBDMEM	osteogenic medium control	-	L-ascorbic acid (100 µM) + β-glycerophosphate (10 mM)
JPC	cocultured untreated 2D-cultured JPCs	JPCs	-
OBJPC	cocultured osteogenically induced 2D-cultured JPCs	osteogenically induced JPCs	L-ascorbic acid (100 µM) + β-glycerophosphate (10 mM)

Note: 10% hPL DMEM/F12 was used to cultivate 2D-cultured JPCs/OBJPCs and their control groups.

“In order to pre-culture THP-1 macrophages, passage 10 of THP-1 cells (4×10^5 cells per chamber) were resuspended in 1.5 mL of 5% hPL RPMI 1640 medium containing 5 nM PMA and seeded into a chamber B on day 5. THP-1 cells were cultured in chamber B for 48 hours to induce M0 macrophage differentiation.” [72]

“On day 7, chamber A and chamber B were assembled to initiate the coculture of 2D-cultured JPCs/OBJPCs and M1/M2 macrophages. After assembling the coculture chamber A and chamber B, they were placed in an adaptor and cocultured for a further five days. For the M1 differentiation, the THP-1-derived M0 macrophages were cultured in a 5% hPL RPMI1640 medium containing 15 ng/mL LPS and 20 ng/mL IFN-γ. Induction of M2 differentiation was achieved in a 5% hPL RPMI1640 medium containing 20 ng/mL IL-4 and 20 ng/mL IL-13. Figure 8 shows the procedure of coculturing of 2D-cultured JPCs/OBJPCs and M1/M2 macrophages.” [72]

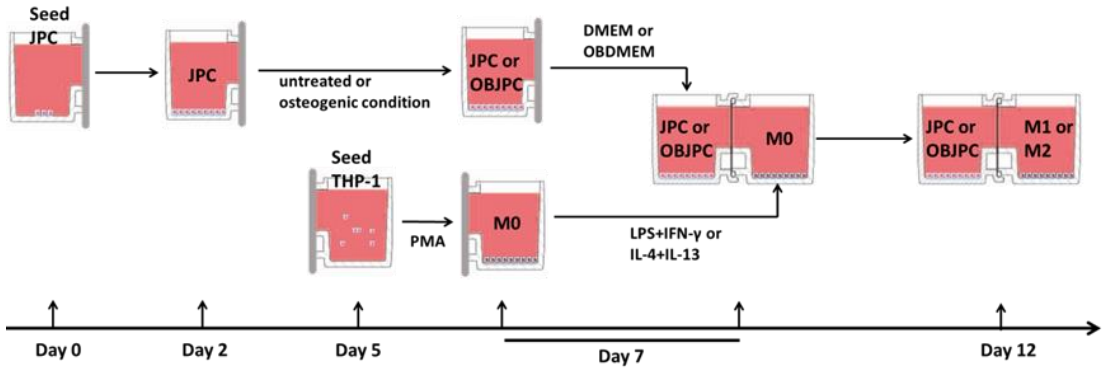

Figure 8. Flow chart of the pre- and co-culturing of 2D-cultured JPCs/OBJPCs and M1/M2 macrophages [72]. (Image published in “He et al., Biomedicines 2021, 9(12), 1753”)

“Cocultures of 2D-JPCs/OBJPCs and M1/M2 macrophages, and their control groups, were cultivated for an additional five days. On day 12, flow cytometry, gene expression, and protein secretion studies for macrophages were performed.

The experimental grouping of cocultured 2D-cultured JPCs/OBJPCs and THP-1-derived M1/M2 macrophages was shown in Figure 9." [72]

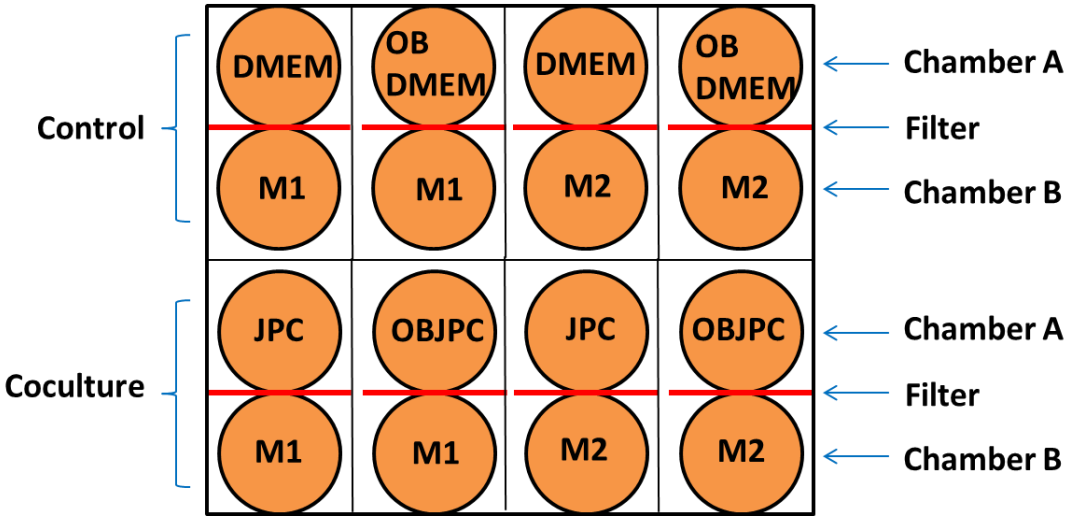

Figure 9. Experimental grouping of the coculture of 2D-cultured JPCs/OBJPCs and M1/M2 macrophages [72]. (Image published in "He et al., Biomedicines 2021, 9(12), 1753")

2.4.3. Horizontal coculture of 3D-cultured JPCs and macrophages

For pre-culturing of 3D-cultured JPCs, the colonialization of β-TCP scaffolds with JPCs was performed in 96-well polypropylene culture plates. Firstly, the β-TCP scaffolds were submerged under 5% hPL DMEM/F12 medium and pre-incubated for 1 hour. Then, passage 4 of 5×10^4 JPCs in 50 µL medium was seeded into the top of each β-TCP scaffold. After 2 hours of incubation, an additional 150 µL DMEM/F12 medium was added into the JPCs-colonized β-TCP scaffold.

After 24 hours of incubation, JPCs-colonialized β-TCP constructs were transferred into new 96-well plates and further grown under untreated conditions (10% hPL DMEM/F12) or osteogenic conditions (10% hPL DMEM/F12 + 100 µM L-ascorbic acid + 10 mM β-glycerophosphate) for ten days (200 µL medium per

construct). Every two days, the medium was changed. In parallel 96-well plates, 200 µL of JPCs-free medium (10% hPL DMEM/F12 with/without osteogenic stimuli) was introduced to the β-TCP scaffold control groups using the identical medium change procedure. In Table 5, we list the abbreviations used for 3D-cultured JPCs/OBJPCs.

Table 5. Used abbreviations for 3D-cultured JPCs/OBJPCs in the coculture groups.

Abbreviation	Group	Cells	Added reagents
TCP	β-TCP scaffold control	-	-
OBTCP	osteogenic β-TCP scaffold control	-	L-ascorbic acid (100 µM) + β-glycerophosphate (10 mM)
3DJPC	cocultured untreated JPCs-colonized β-TCP scaffold	JPCs	-
3DOBJPC	cocultured osteogenically induced JPCs-colonized β-TCP scaffold	osteogenically induced JPCs	L-ascorbic acid (100 µM) + β-glycerophosphate (10 mM)

Note: 10% hPL DMEM/F12 was used to cultivate 3D-cultured JPCs/OBJPCs and their control groups.

To pre-culture THP-1 macrophages, passage 13 of THP-1 cells (4×10^5 cells per chamber) resuspended in 1.5 mL of 5% hPL RPMI 1640 medium were introduced into chamber B on day 9. PMA in a concentration of 5 nM was used to induce

THP-1 cells to differentiate into M0 macrophages from day 9 to day 11.

On day 11, the assembly of the coculture of 3DJPCs/3DOBJPCs and M1/M2 macrophages was performed. For the coculture groups, untreated or osteogenically induced JPCs/OBJPCs-colonialized scaffolds (five blocks of constructs per chamber) were transferred into chamber A containing 1.3 mL of 10% hPL DMEM/F12 medium. For the scaffold controls, five blocks of cell-free TCP/OBTCP scaffolds were transferred into the corresponding control chamber A. In chamber B, for the differentiation of M1, THP-1 differentiated M0 macrophages were cultured in 1.5 mL of 5% hPL RPMI1640 medium containing 15 ng/mL LPS and 20 ng/mL IFN-γ. In order to induce M2 macrophages, 20 ng/mL IL-4 and 20 ng/mL IL-13 were used as stimuli. Figure 10 shows the procedure of coculturing of 3DJPCs/3DOBJPCs and M1/M2 macrophages.

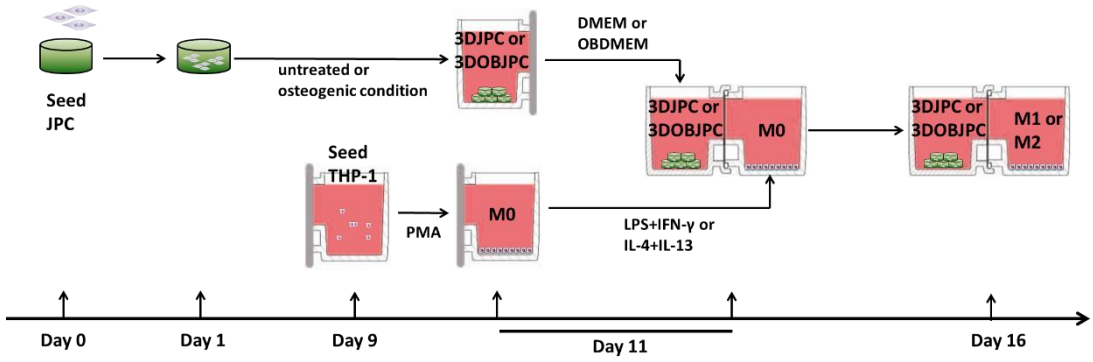

Figure 10. Flow chart of the pre- and co-culturing of 3D-cultured JPCs/OBJPCs and M1/M2 macrophages.

The assembled coculture chambers were subsequently set into a 96-well plate-size adapter and further incubation was performed. The 3DJPCs/3DOBJPCs + M1/M2 coculture groups and the TCP/OBTCP + M1/M2 scaffold control groups were cultured for an additional five days. Gene expression measurements of

M1/M2 macrophages in the coculture system were performed on day 16. The experimental grouping of cocultures of 3DJPCs/3DOBJPCs and M1/M2 macrophages is illustrated in Figure 11.

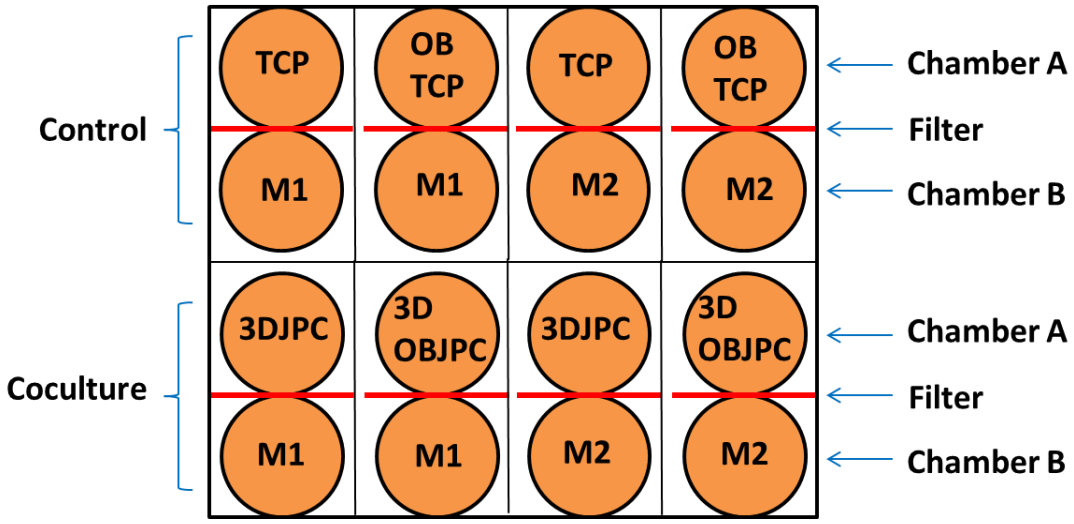

Figure 11. Experimental grouping of cocultures of 3D-cultured JPCs/OBJPCs and M1/M2 macrophages.

2.5. Flow cytometric analyses of resulting THP-1-derived macrophages

“After five days of coculture with 2D-cultured JPCs/OBJPCs and M1/M2 in the horizontal coculture system, the cocultured THP-1-derived macrophages were removed from the horizontal plate using TrypLE-Express, and cell surface markers specific for M1 or M2 were discovered using flow cytometry. In subsequent sample preparation steps, cells were centrifuged (1400 rpm for 5 minutes) and the supernatants were removed. Cell pellets were then resuspended in 10 % Gamunex and kept on ice for 15 minutes. The cells were then treated in the dark for 30 minutes with flow cytometric antibodies. After two washes with FACs buffer (PBS + 0.1 % BSA + 0.1 % sodium azide), cells were measured using the Guava EasyCyte 6HT-2L flow cytometer. The FlowJo

program was utilized for data visualization. Table 6 shows the antibodies used in the flow cytometry measurement.” [72]

Table 6. List of antibodies used in the flow cytometry [72]. (Table published in “He et al., Biomedicines 2021, 9(12), 1753”)

Human Antigen (Clone)	Conjugate/Isotype control
CD80 (2D10)	PE/IgG1
CD86 (BU63)	PE/IgG1
CD11b (ICRF44)	PE/IgG1
HLA-DR (L243)	APC/IgG2a
CD209 (9E9A8)	APC/IgG2a
CD197 (G043H7)	APC/IgG2a
CD36 (5–271)	APC/IgG2a
CD14 (M5E2)	APC/IgG2a

2.6. Quantitative gene expression analysis of THP-1-derived macrophages

The quantitative PCR method was used to investigate the gene expressions of M1 and M2 macrophages cocultured with 2D- and 3D-cultured JPCs/OBJPCs in the horizontal coculture system.

“In the coculture of 2D-cultured JPCs/OBJPCs and M1/M2, total RNA was isolated from M1 or M2 macrophages using the NucleoSpin RNA kit following the manufacturer's recommendations. NanoDrop One instrument was used to figure out the concentration and purity of RNA. A total of 100 ng of RNA were used for the purpose of synthesizing cDNA and the SuperScript VILO Kit instructions were followed. The real-time LightCycler System was used to measure mRNA expression levels in the samples of different groups. The primer kits from Search LC company and a DNA master SYBR Green I kit were used for 40 amplification

cycles of the CD163, CD209, TNF-α, CCL5, IL-6, IL-10 or CXCR4 DNA. The housekeeping gene GAPDH was used as a standard to normalize transcript levels of target genes. To evaluate and report the findings, we set the gene ratio in the M1/M2 monoculture group to 1 (control) and calculated x-fold induction indices compared to this control." [72]

For coculture of 3DJPCs/3DOBJPCs and M1/M2 macrophages, the NucleoSpin RNA kit was also used for the total RNA isolation of macrophages. After quantification by the NanoDrop One, cDNA was synthesized using 100 ng of RNA according to the LunaScript® RT SuperMix Kit instructions. The mRNA expression levels were measured by the QuantStudio 3 Real-Time PCR Instrument. DEPC-treated water, Luna® Universal Probe qPCR Master Mix, and primers of the targeted gene (CD163, CD209, TNF-α, CD36 or IL-10) from Integrated DNA Technologies were used for 40 amplification cycles of the synthesized cDNA. Transcript levels of the target genes were normalized to the housekeeping gene GAPDH. The M1/M2 monoculture TCP group was set to control, and the delta-delta Ct ($\Delta\Delta$Ct) method was used to calculate the relative mRNA levels.

2.7. Analysis of cytokine and chemokine release of macrophages/JPCs in the horizontal coculture system

"Human cytokine proteome profiler array kits were utilized to quantify cytokine/chemokine secretion in the supernatants of M1 or M2 macrophages following five days of horizontal coculture with 2D-cultured JPCs/OBJPCs. The membranes of the proteome profiler were blocked in array buffer for 1 hour at room temperature and then treated overnight at 4 °C with sample supernatants and antibody combinations. Following three washes, the membranes were treated with diluted streptavidin–HRP at room temperature for thirty minutes. After three washes again, the membranes were treated with a 1 mL chemiluminescent reagent combination and subjected to radiographic images for ten minutes. Positive signals or dots were analysed after scanning the generated x-ray films." [72]

2.8. Statistical analysis

The measured data were expressed as mean ± standard error of the mean (mean ± SEM), and statistical analyses were performed and visualized by GraphPad Prism software. Student’s t-test or one-way analysis of variance (ANOVA) followed by Tukey's multiple comparison test was used. The values of $p < 0.05$ were considered statistically significant.

3. Results

3.1. Cell surface markers expression of macrophages in the direct coculture model (This section published in “He et al., International journal of molecular sciences, 2021, 22(9): 4310”)

“In the JPCs and macrophages contact coculture system, for the flow cytometric investigation of CD marker expression on M1 macrophages, CD68 positive cells were gated to distinguish THP-1 macrophages in the detached cell suspension. The expression of CD80 was applied to measure the polarization of M0 to M1 macrophages. In comparison to monoculture M1-Control group, the M1-JPC coculture group had considerably lower percentages of $CD68^{+}CD80^{+}$ positive cells (M1-Control 47.34 ± 0.92 versus M1-JPC 2.64 ± 0.32, $p < 0.05$) (Figure 12).” [71]

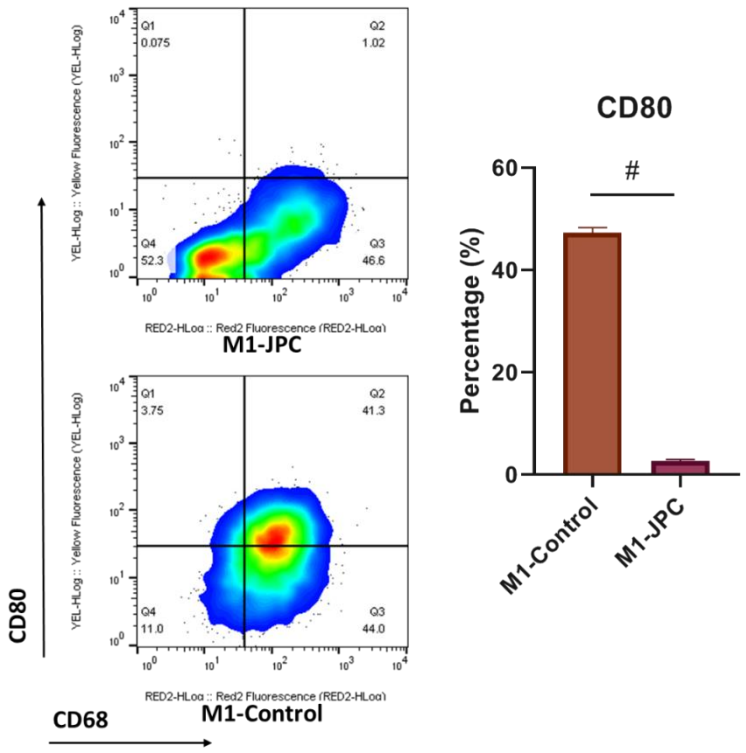

Figure 12. CD80 expression in CD68$^+$ macrophages in monoculture (M1-Control) and coculture (M1-JPC) groups is shown by the representative flow cytometry dot plots and the histogram [71]. Means ± standard error of the mean were determined and the results were compared using Student's t-test (n = 3, $^{\#}$ p < 0.05). (Image published in "He et al., International journal of molecular sciences, 2021, 22(9): 4310")

"To investigate the cell surface CD markers expression on cocultured M2 macrophages in the contact coculture system, CD68$^+$ cells were gated to identify macrophages, and CD206$^+$ and CD163$^+$ cells were utilized to assess the polarization of M2 macrophages. The M2-JPC coculture group had a higher proportion of CD68$^+$CD163$^+$ cells than the monoculture M2-Control group (M2-Control 0.08 ± 0.02 versus M2-JPC 1.22 ± 0.10, p < 0.05). The coculture group had an increasing tendency of CD68$^+$CD206$^+$ than the monoculture control group (Figure 13)." [71]

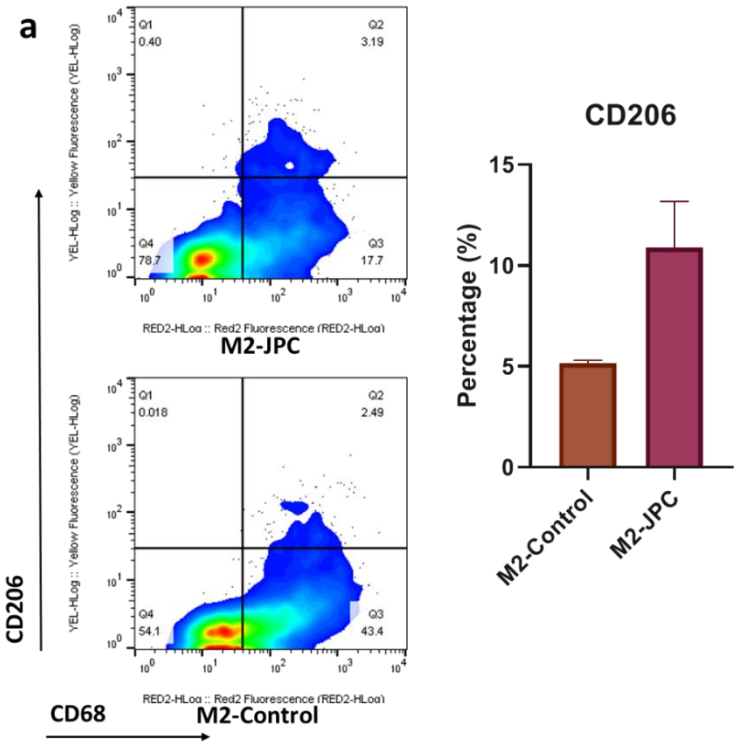

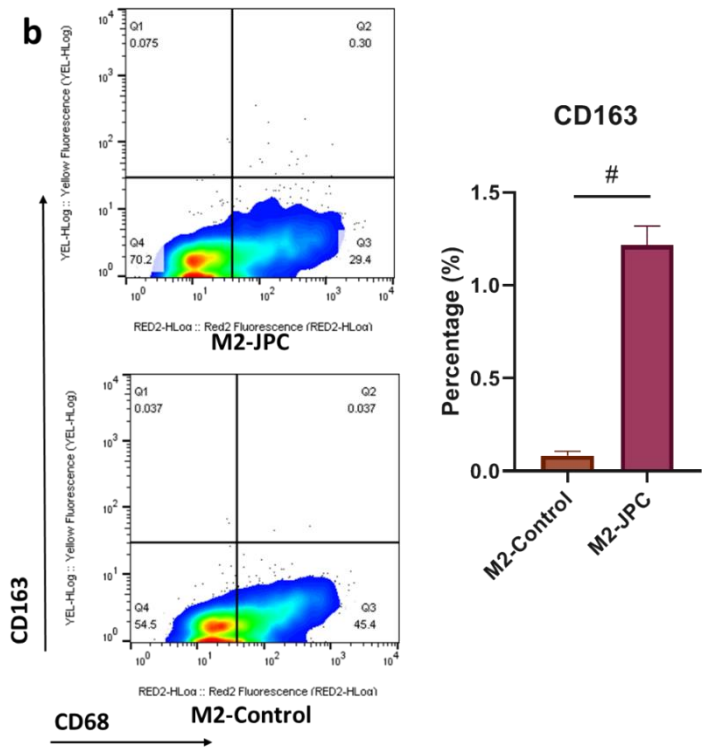

Figure 13. CD206 (a) and CD163 (b) expression in CD68^{+} macrophages in monoculture (M2-Control) and coculture (M2-JPC) groups, as shown by the representative flow cytometry dot plots and the histogram [71]. Means ± standard error of the mean were determined and the results were compared using Student's t-test (n = 3, $^{\#}$ $p < 0.05$). (Image published in "He et al., International journal of molecular sciences, 2021, 22(9): 4310")

3.2. Cell surface markers expression of macrophages cocultured with 2D-cultured JPCs/OBJPCs in the horizontal coculture system (This section published in "He et al., Biomedicines 2021, 9(12), 1753")

3.2.1. Surface marker expression on M1 macrophages cocultured with 2D-cultured JPCs/OBJPCs in the horizontal coculture system

"After five days of horizontal coculture, flow cytometry was used to examine the cell surface markers of M1 or M2 macrophages to determine the influence of 2D-cultured JPCs/OBJPCs on macrophage polarization." [72]

“The flow cytometry results of cell surface marker expression on M1 macrophages are presented in Figure 14. The percentages of $CD80^+$, $CD86^+$, $HLA\text{-}DR^+$ and $CD197^+$ cells in JPCs/OBJPCs-M1 coculture groups were obviously downregulated compared with those in the DMEM/OBDMEM-M1 control groups. On the contrary, compared with the DMEM/OBDMEM-M1 groups, the percentages of $CD14^+$ cells were obviously higher in JPCs/OBJPCs-M1 groups. The data of measurements are displayed in Table 7.” [72]

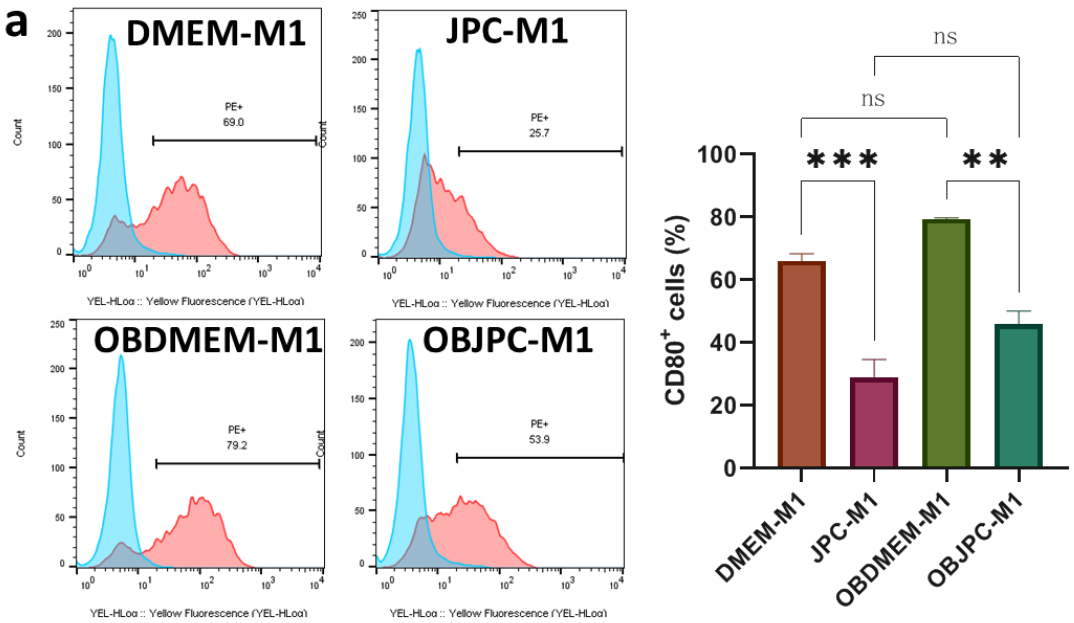

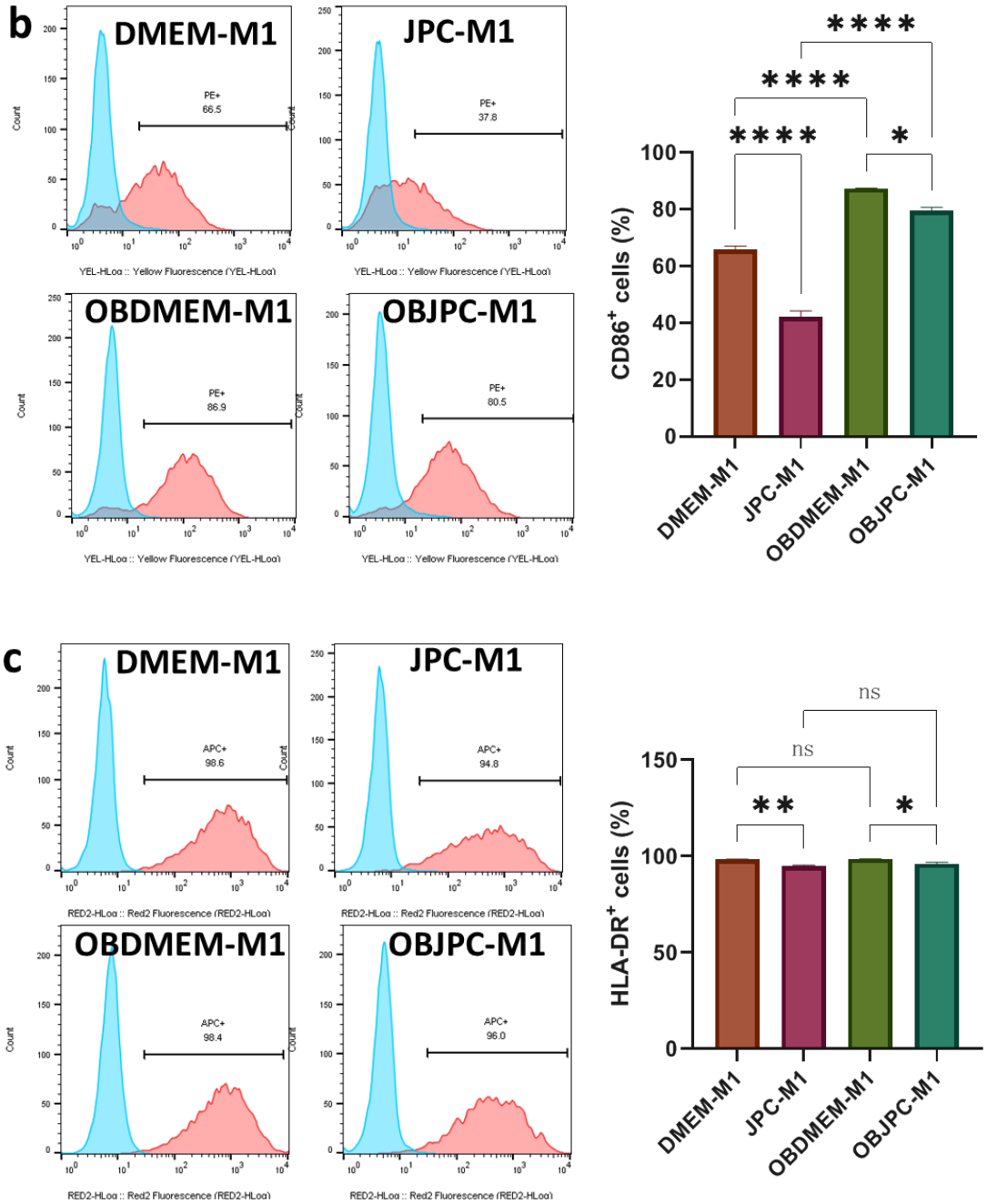
b
DMEM-M1
PE+
66.5
JPC-M1
PE+
37.8
OBDMEM-M1
PE+
86.9
OBJPC-M1
PE+
80.5
Count
YEL-HLoa :: Yellow Fluorescence (YEL-HLoa)
CD86+ cells (%)
****
****
****
*
DMEM-M1
JPC-M1
OBDMEM-M1
OBJPC-M1
c
DMEM-M1
APC+
98.6
JPC-M1
APC+
94.8
OBDMEM-M1
APC+
98.4
OBJPC-M1
APC+
96.0
RED2-HLoa :: Red2 Fluorescence (RED2-HLoa)
HLA-DR+ cells (%)
ns
ns
**
*
DMEM-M1
JPC-M1
OBDMEM-M1
OBJPC-M1

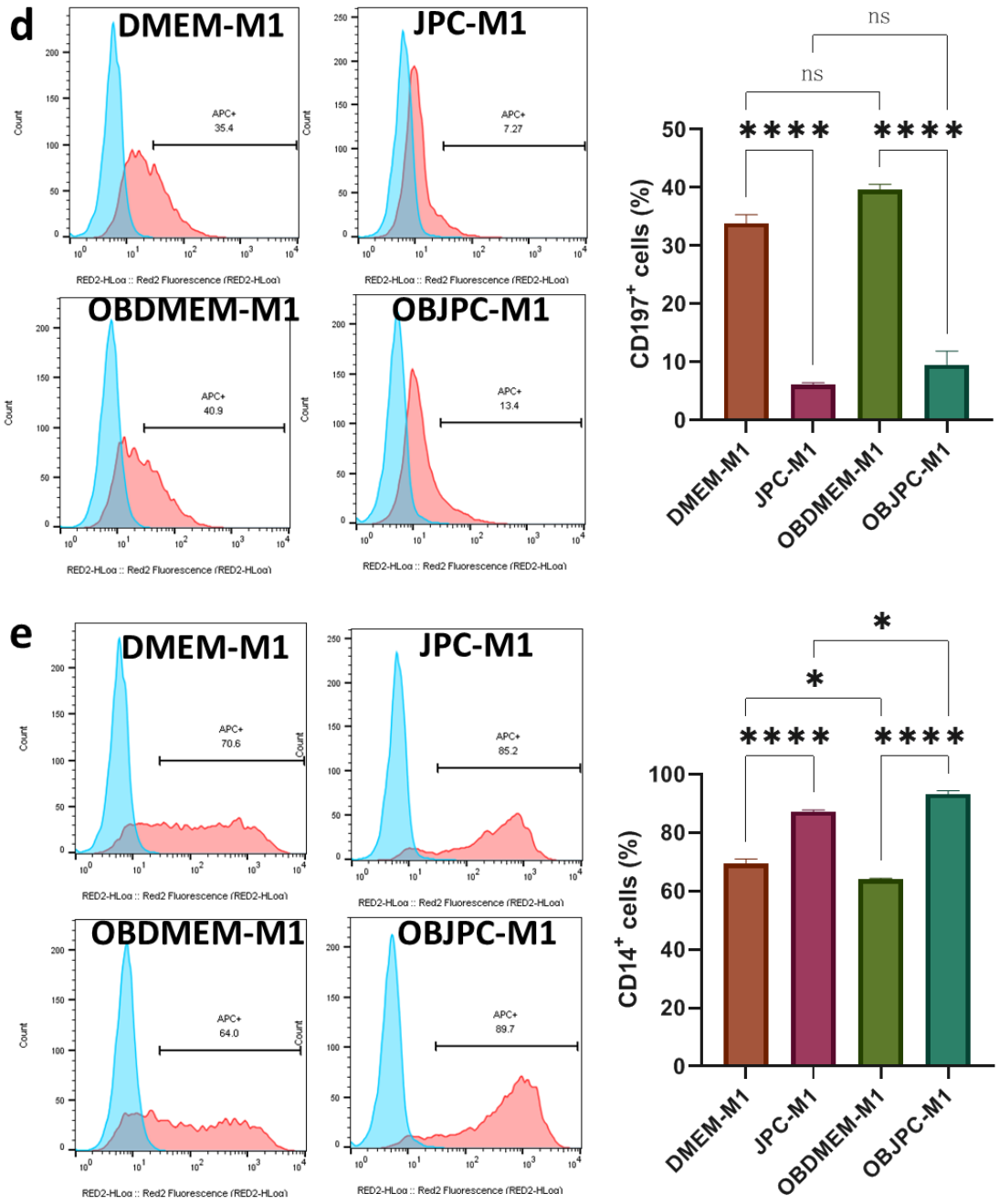
d
DMEM-M1
APC+
35.4
JPC-M1
APC+
7.27
OBDMEM-M1
APC+
40.9
OBJPC-M1
APC+
13.4
Count
RED2-HLoa :: Red2 Fluorescence (RED2-HLoa)
ns
ns
****
****
CD197+ cells (%)
DMEM-M1
JPC-M1
OBDMEM-M1
OBJPC-M1
e
DMEM-M1
APC+
70.6
JPC-M1
APC+
85.2
OBDMEM-M1
APC+
64.0
OBJPC-M1
APC+
89.7
*
*
****
****
CD14+ cells (%)
DMEM-M1
JPC-M1
OBDMEM-M1
OBJPC-M1

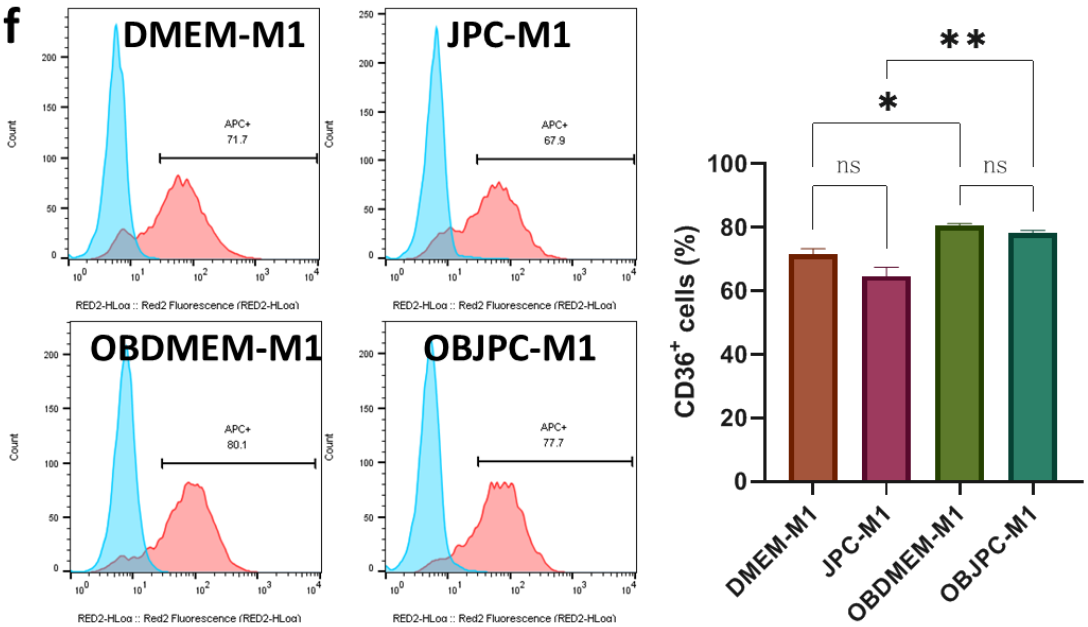

Figure 14. Representative single parameter histograms and quantitative analysis of CD80 (a), CD86 (b), HLA-DR (c), CD197 (d), CD14 (e) and CD36 (f) expression on M1 macrophages cocultured with 2D-cultured JPCs/OBJPCs in the horizontal coculture system as detected by flow cytometry [72]. Means ± standard error of the mean were calculated and analyzed using one-way analysis of variance (n = 3, * $p < 0.05$, ** $p < 0.01$, *** $p < 0.001$, **** $p < 0.0001$). (Images published in "He et al., Biomedicines 2021, 9(12), 1753")

Table 7. Percentage of M1 macrophages that are positive for CD markers when cocultured with 2D-cultured JPCs/OBJPCs [72]. (Table published in "He et al., Biomedicines 2021, 9(12), 1753")

Markers	DMEM-M1	JPC-M1	OBDMEM-M1	OBJPC-M1
CD80	66.12 ± 2.24	28.87 ± 5.84 [a]	79.46 ± 0.29	45.91 ± 4.18 [b]
CD86	65.68 ± 1.40	42.05 ± 2.14 [a]	87.26 ± 0.22	79.45 ± 1.22 [b]
HLA-DR	98.33 ± 0.25	94.98 ± 0.48 [a]	98.57 ± 0.08	96.18 ± 0.70 [b]
CD197	33.87 ± 1.47	6.15 ± 0.31 [a]	39.61 ± 0.97	9.56 ± 2.35 [b]
CD14	69.45 ± 1.63	87.22 ± 0.54 [a]	64.01 ± 0.48	93.20 ± 1.16 [b]
CD36	71.53 ± 1.80	64.59 ± 2.86	80.42 ± 0.77	78.21 ± 0.84

[a] The DMEM-M1 and the JPC-M1 groups showed significant differences ($p < 0.05$); [b] The OBDMEM-M1 and the OBJPC-M1 groups showed significant differences ($p < 0.05$) (means ± standard error of the mean).

3.2.2. Surface marker expression on M2 macrophages cocultured with 2D-cultured JPCs/OBJPCs in the horizontal coculture system

"The flow cytometry results of surface marker expression on M2 macrophages are presented in Figure 15. Compared with the OBDMEM-M2 group, the percentages of $CD209^+$, $CD11b^+$ and $CD14^+$ cells were significantly higher in the OBJPC-M2 group. Similarly, in comparison to the DMEM-M2 control group, a tendency to increase the expression of the above-mentioned CD markers was observed in the JPC-M2 coculture group. Additionally, compared with the DMEM/OBDMEM-M2 groups, the percentages of $CD86^+$ cells were significantly downregulated in the JPC/OBJPC-M2 groups. The data of measurements are displayed in Table 8." [72]

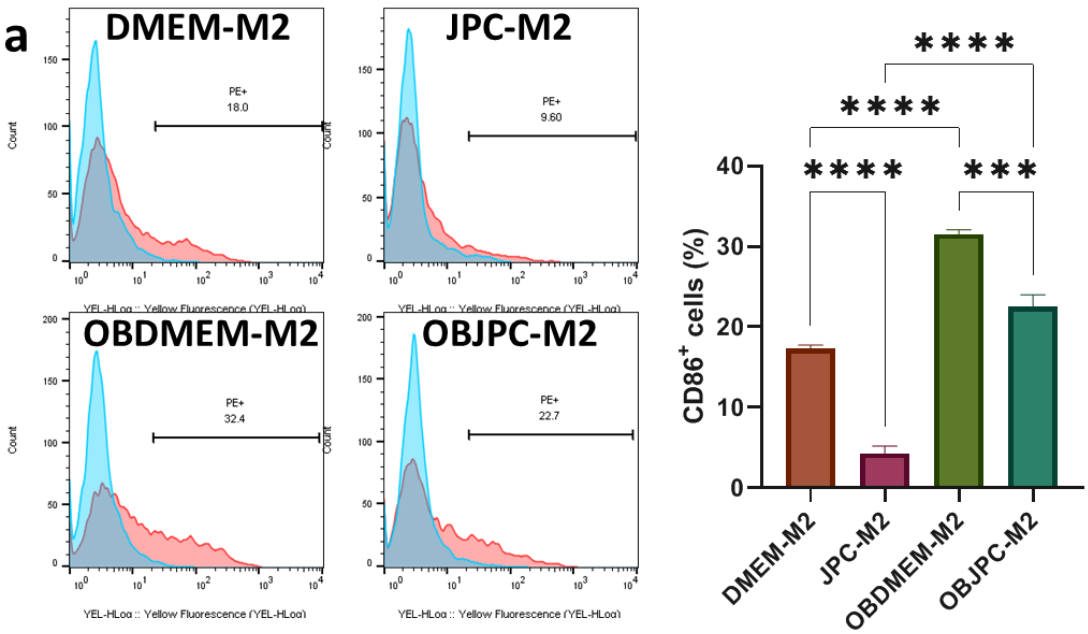

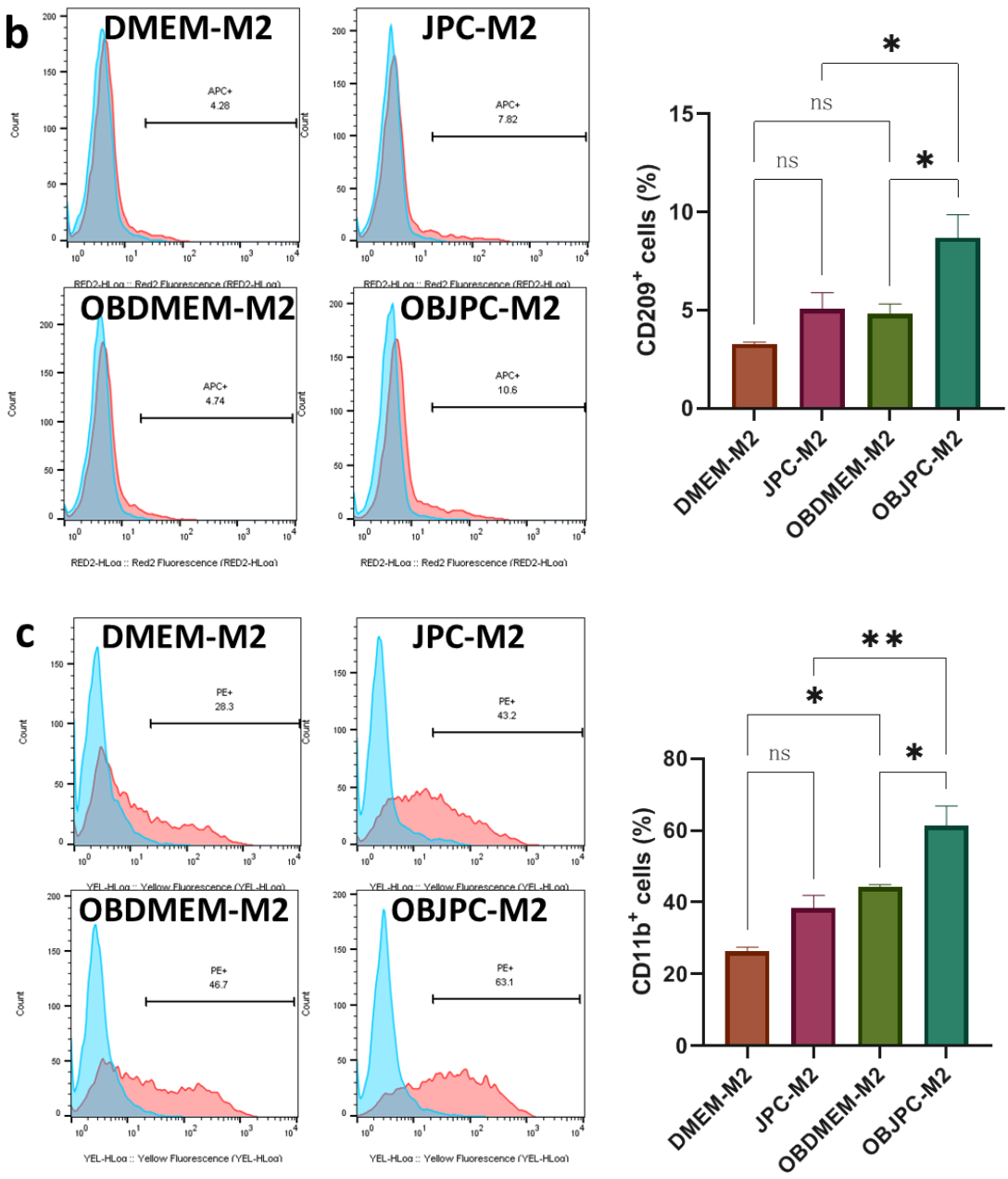
b
DMEM-M2
APC+
4.28
JPC-M2
APC+
7.82
OBDMEM-M2
APC+
4.74
OBJPC-M2
APC+
10.6
Count
RED2-HLog :: Red2 Fluorescence (RED2-HLog)
CD209+ cells (%)
ns
ns
*
*
DMEM-M2
JPC-M2
OBDMEM-M2
OBJPC-M2
c
DMEM-M2
PE+
28.3
JPC-M2
PE+
43.2
OBDMEM-M2
PE+
46.7
OBJPC-M2
PE+
63.1
YEL-HLog :: Yellow Fluorescence (YEL-HLog)
CD11b+ cells (%)
**
*
ns
*
DMEM-M2
JPC-M2
OBDMEM-M2
OBJPC-M2

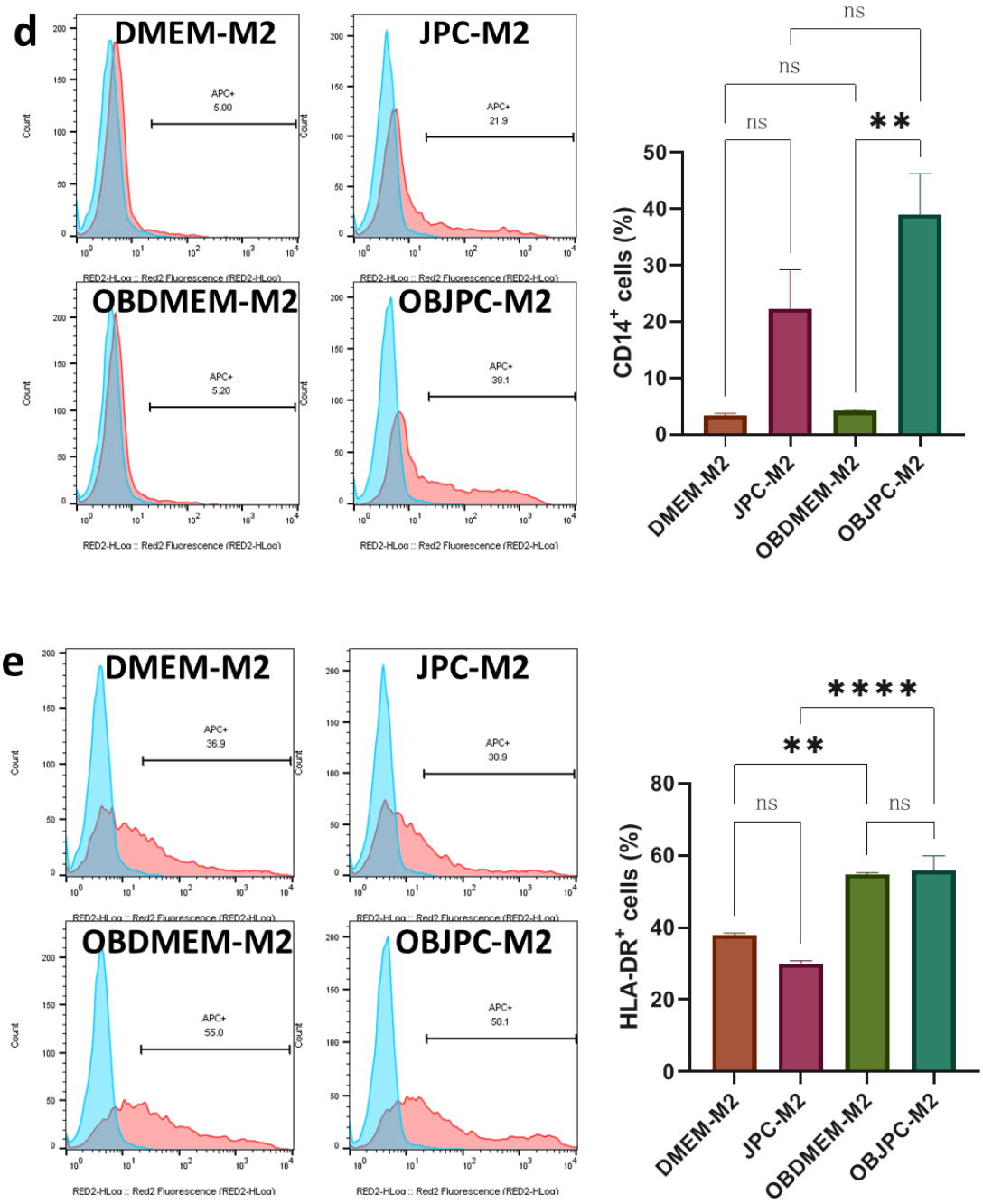
d
DMEM-M2
APC+
5.00
JPC-M2
APC+
21.9
OBDMEM-M2
APC+
5.20
OBJPC-M2
APC+
39.1
Count
RED2-HLog :: Red2 Fluorescence (RED2-HLog)
ns
ns
ns
**
CD14+ cells (%)
DMEM-M2
JPC-M2
OBDMEM-M2
OBJPC-M2
e
DMEM-M2
APC+
36.9
JPC-M2
APC+
30.9
OBDMEM-M2
APC+
55.0
OBJPC-M2
APC+
50.1
****
**
ns
ns
HLA-DR+ cells (%)

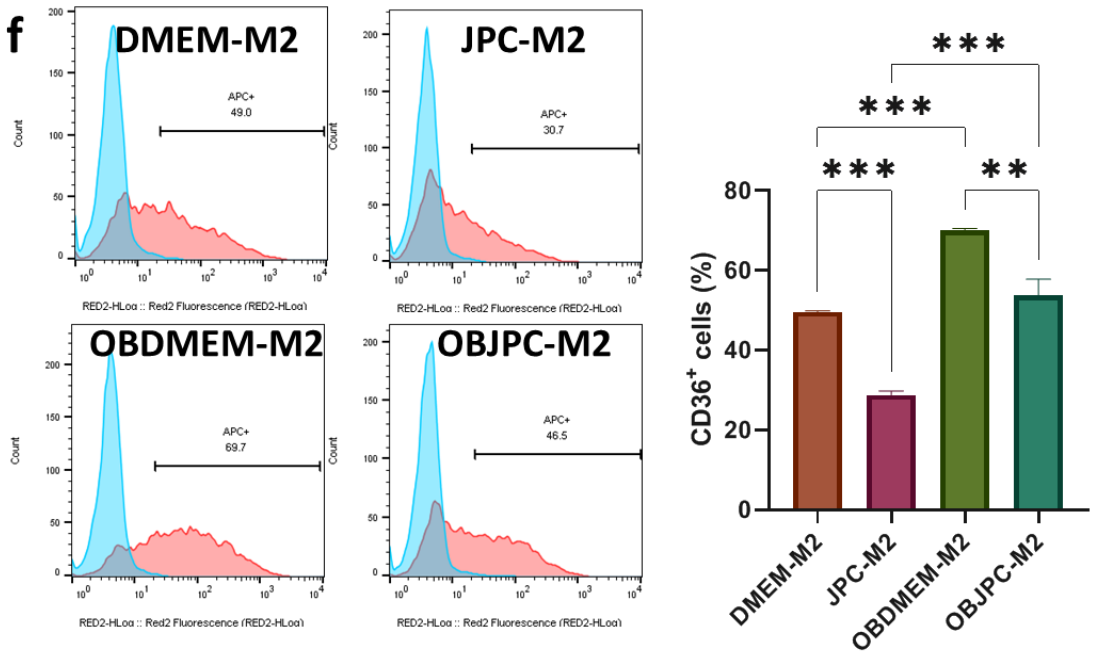

Figure 15. Representative single parameter histograms and quantitative analysis of CD86 (a), CD209 (b), CD11b (c), CD14 (d), HLA-DR (e) and CD36 (f) expression on M2 macrophages co-cultivated with JPCs/OBJPCs in the horizontal coculture system as detected by flow cytometry [72]. Means ± standard error of the mean were determined and analyzed using one-way analysis of variance (n = 3, * $p < 0.05$, ** $p < 0.01$, *** $p < 0.001$, **** $p < 0.0001$). (Images published in "He et al., Biomedicines 2021, 9(12), 1753")

Table 8. Percentage of M2 macrophages that are positive for CD markers when cocultured with 2D-cultured JPCs/OBJPCs [72]. (Table published in "He et al., Biomedicines 2021, 9(12), 1753")

Markers	DMEM-M2	JPC-M2	OBDMEM-M2	OBJPC-M2
CD86	17.33 ± 0.43	4.29 ± 0.93 [a]	31.54 ± 0.53	22.51 ± 1.50 [b]
CD209	3.29 ± 0.10	5.06 ± 0.83	4.81 ± 0.51	8.68 ± 1.19 [b]
CD11b	26.37 ± 1.15	38.39 ± 3.53	44.23 ± 0.73	61.39 ± 5.43 [b]
CD14	3.37 ± 0.34	22.30 ± 6.88	4.16 ± 0.26	39.01 ± 7.20 [b]
HLA-DR	37.95 ± 0.51	29.97 ± 0.79	54.74 ± 0.49	55.88 ± 4.02
CD36	49.51 ± 0.33	28.78 ± 0.97 [a]	70.05 ± 0.43	53.63 ± 4.11 [b]

[a] The DMEM-M2 and the JPC-M2 groups showed significant differences ($p < 0.05$); [b] The OBDMEM-M2 and the OBJPC-M2 groups showed significant differences ($p < 0.05$) (means ± standard error of the mean).

3.3. Gene expression analysis of macrophages in the horizontal coculture system

3.3.1. Gene expression of macrophages cocultured with 2D-cultured JPCs/OBJPCs (This section published in "He et al., Biomedicines 2021, 9(12), 1753")

"A quantitative PCR analysis of the CD163, CD209, TNF-α, CCL5, IL-6, IL-10, CXCR4 and IL-6 gene expression in the horizontally cocultured M1 or M2 macrophages was performed to investigate the influence of 2D-cultured JPCs/OBJPCs on macrophage polarization." [72]

"Gene expression results of the cocultured M1 macrophages are presented in Figure 16. CD163 and CD209 gene expressions were considerably elevated in the JPC-M1 group when compared with the DMEM-M1 group. Additionally, the expression level of the CD163 gene in the OBJPC-M1 group was obviously increased compared with that in the OBDMEM-M1 group. Contrary to this, the expression of CCL5 gene in JPC/OBJPC-M1 groups was obviously decreased compared with the detected level in the DMEM/OBDMEM-M1 control groups. Furthermore, when compared to the DMEM-M1 and OBDMEM-M1 groups, TNF-α gene expression in the JPCs-M1 and OBJPCs-M1 groups tended to be downregulated, whereas IL-10 gene expression tended to be upregulated. The data of measurements are displayed in Table 9." [72]

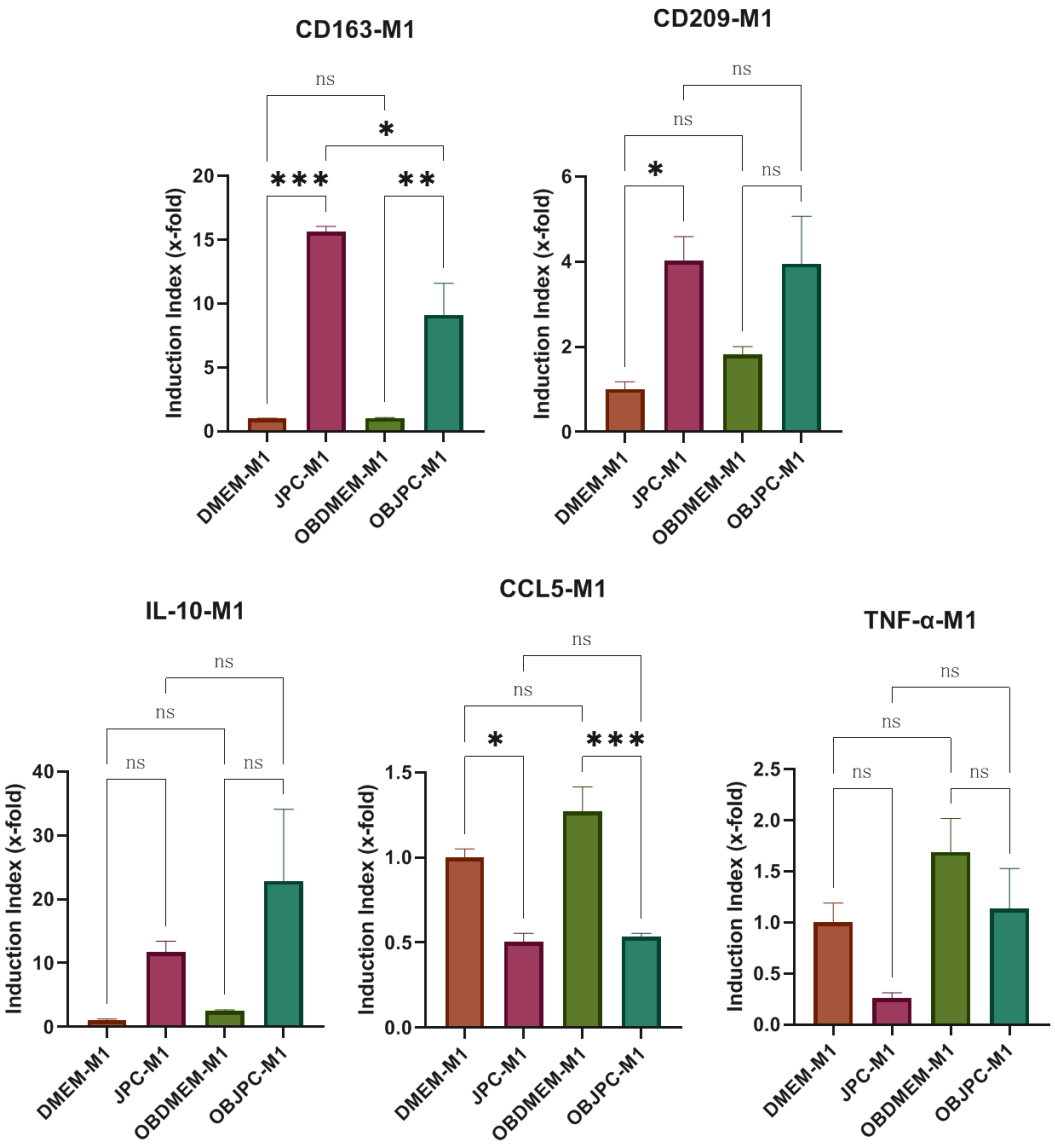

Figure 16. CD163, CD209, IL-10, CCL5 and TNF-α gene expression of M1 macrophages cocultured with 2D-cultured JPCs/OBJPCs [72]. Means ± standard error of the mean were calculated and analyzed using one-way analysis of variance (n = 3, * $p < 0.05$, ** $p < 0.01$, *** $p < 0.001$). (Images published in "He et al., Biomedicines 2021, 9(12), 1753")

Table 9. Gene expression of the M1 macrophages cocultured with 2D-cultured JPCs/OBJPCs [72]. (Table published in "He et al., Biomedicines 2021, 9(12), 1753")

Genes	DMEM-M1	JPC-M1	OBDMEM-M1	OBJPC-M1

CD163	1.00 ± 0.03	15.62 ± 0.42 [a]	1.03 ± 0.04	9.12 ± 2.48 [b]
CD209	1.00 ± 0.18	4.02 ± 0.57 [a]	1.81 ± 0.20	3.95 ± 1.11
IL-10	1.00 ± 0.25	11.70 ± 1.71	2.48 ± 0.20	22.88 ± 11.20
CCL5	1.00 ± 0.05	0.50 ± 0.05 [a]	1.27 ± 0.14	0.53 ± 0.02 [b]
TNF-α	1.00 ± 0.19	0.27 ± 0.06	1.69 ± 0.33	1.14 ± 0.39

[a] The DMEM-M1 and the JPC-M1 groups showed significant differences ($p < 0.05$); [b] The OBDMEM-M1 and the OBJPC-M1 groups showed significant differences ($p < 0.05$) (means ± standard error of the mean).

“Gene expression results of cocultured M2 macrophages are presented in Figure 17. Coculture group JPC-M2 showed an upregulated tendency in IL-6 gene expression compared with the control group DMEM-M2. Compared with the OBMEM-M2 control group, the IL-6 gene expression level was significantly higher in the OBJPC-M2 group. In the OBJPC-M2 coculture group, CD163, IL-10 and CD209 gene expressions were found to have an upregulated tendency when compared with those in the OBDMEM-M2 control group. The data of measurements are displayed in Table 10.” [72]

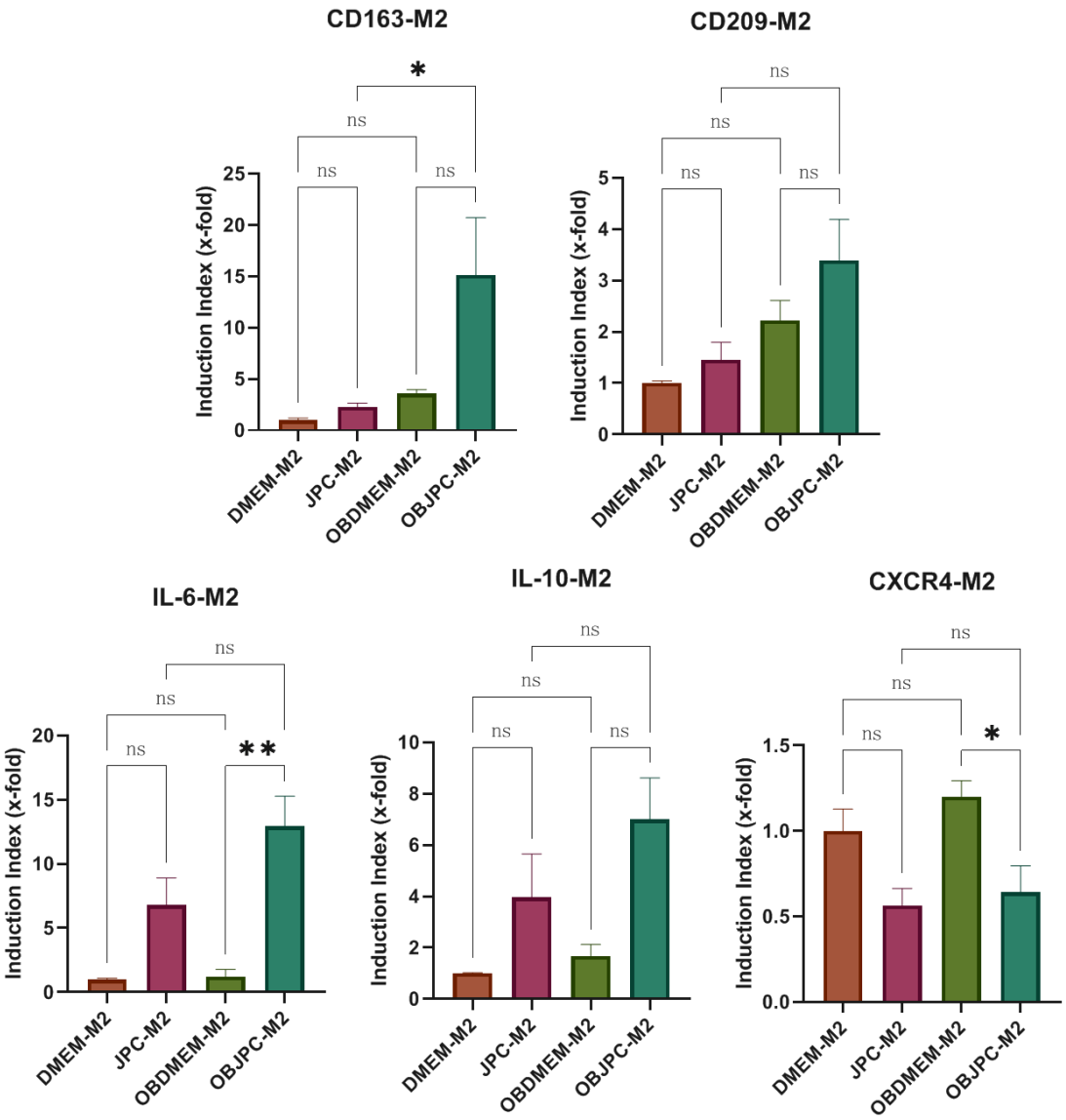

Figure 17. CD163, CD209, IL-6, IL-10 and CXCR4 gene expression of M2 macrophages cocultured with 2D-cultured JPCs/OBJPCs [72]. Means ± standard error of the mean were calculated and analyzed using one-way analysis of variance (n = 3, * $p < 0.05$, ** $p < 0.01$, *** $p < 0.001$). (Images published in "He et al., Biomedicines 2021, 9(12), 1753")

Table 10. Gene expression of the M2 macrophages cocultured with 2D-cultured JPCs/OBJPCs [72]. (Table published in "He et al., Biomedicines 2021, 9(12), 1753")

Genes	DMEM-M2	JPC-M2	OBDMEM-M2	OBJPC-M2
CD163	1.00 ± 0.21	2.27 ± 0.38	3.60 ± 0.37	15.13 ± 5.60
CD209	1.00 ± 0.05	1.45 ± 0.35	2.23 ± 0.38	3.39 ± 0.80
IL-6	1.00 ± 0.08	6.82 ± 2.09	1.22 ± 0.56	12.93 ± 2.34 [b]
IL-10	1.00 ± 0.03	3.96 ± 1.70	1.67 ± 0.46	7.01 ± 1.60
CXCR4	1.00 ± 0.13	0.56 ± 0.10	1.20 ± 0.09	0.64 ± 0.16 [b]

[a] The DMEM-M2 and the JPC-M2 groups showed significant differences ($p < 0.05$); [b] The OBDMEM-M2 and the OBJPC-M2 groups showed significant differences ($p < 0.05$) (means ± standard error of the mean).

3.3.2. Gene expression of macrophages cocultured with 3D-cultured JPCs/OBJPCs

To assess the effects of 3D-cultured JPCs/OBJPCs (3DJPCs/3DOBJPCs) on M1/M2 macrophage polarization, the gene expression analysis of TNF-α, CD163, IL-10, CD209 and CD36 in the horizontally cocultured M1 or M2 macrophages was evaluated by PCR.

The qPCR results of cocultured M1 macrophages with the JPC-seeded 3D constructs (3DOBJPC) are presented in Figure 18. The TNF-α gene expression of M1 macrophages in the 3DJPC/3DOBJPC-M1 groups was obviously downregulated compared with that in the TCP-M1/OBTCP-M1 groups. CD163 gene expression in the 3DJPC-M1 group was significantly increased compared to that detected in the TCP-M1 group. Besides, compared to the TCP-M1 control group, CD209 tended to be increased in the 3DJPC-M1 group. The data of measurements are displayed in Table 11.

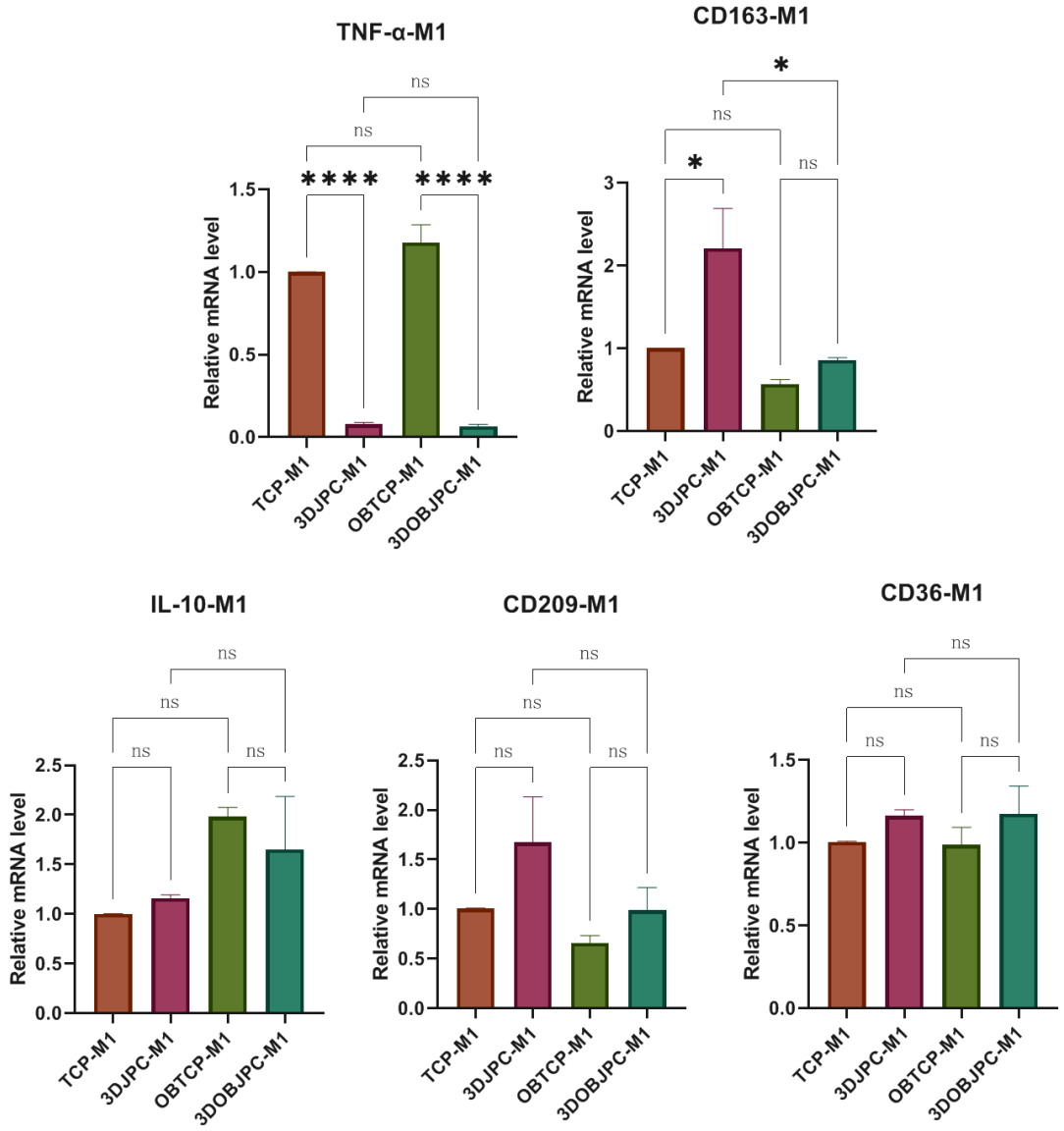

Figure 18. TNF-α, CD163, IL-10, CD209 and CD36 gene expression of M1 macrophages cocultured with 3DJPCs/3DOBJPCs. Means ± standard error of the mean were calculated and analyzed using one-way analysis of variance (n = 3, * $p < 0.05$, **** $p < 0.0001$).

Table 11. Gene expression of M1 macrophages cocultured with 3D-cultured JPCs/OBJPCs.

Genes	TCP-M1	3DJPC-M1	OBTCP-M1	3DOBJPC-M1

TNF-α	1.00 ± 0.00	0.08 ± 0.01 [a]	1.18 ± 0.11	0.07 ± 0.01 [b]
IL-10	1.00 ± 0.00	1.16 ± 0.04	1.98 ± 0.09	1.65 ± 0.54
CD163	1.01 ± 0.00	2.21 ± 0.48 [a]	0.57 ± 0.06	0.86 ± 0.03
CD209	1.01 ± 0.00	1.67 ± 0.46	0.66 ± 0.07	0.99 ± 0.23
CD36	1.01 ± 0.00	1.17 ± 0.04	0.99 ± 0.11	1.18 ± 0.17

[a] The TCP-M1 and the 3DJPC-M1 groups showed significant differences ($p < 0.05$); [b] The OBTCP-M1 and the 3DOBJPC-M1 groups showed significant differences ($p < 0.05$) (means ± standard error of the mean).

In M2 macrophages cocultured with 3D-cultured JPCs/OBJPCs, compared with the TCP/OBTCP-M2 scaffold control groups, the gene expression of TNF-α and CD163 were in the tendency downregulated and upregulated, respectively. The gene expression of IL-10 in the 3DJPC-M2 group was obviously increased compared with that in the TCP-M2 group. The CD209 gene expression of M2 was shown to be significantly increased in 3DJPC/3DOBJPC-M2 groups when compared with the TCP-M2/OBTCP-M2 groups. Furthermore, compared to the OBTCP-M2 scaffold control group, CD36 was downregulated in the 3DOBJPC-M2 group. Gene expression results of cocultured M2 macrophages with the 3DJPC-groups are presented in Figure 19. The data of measurements are displayed in Table 12.

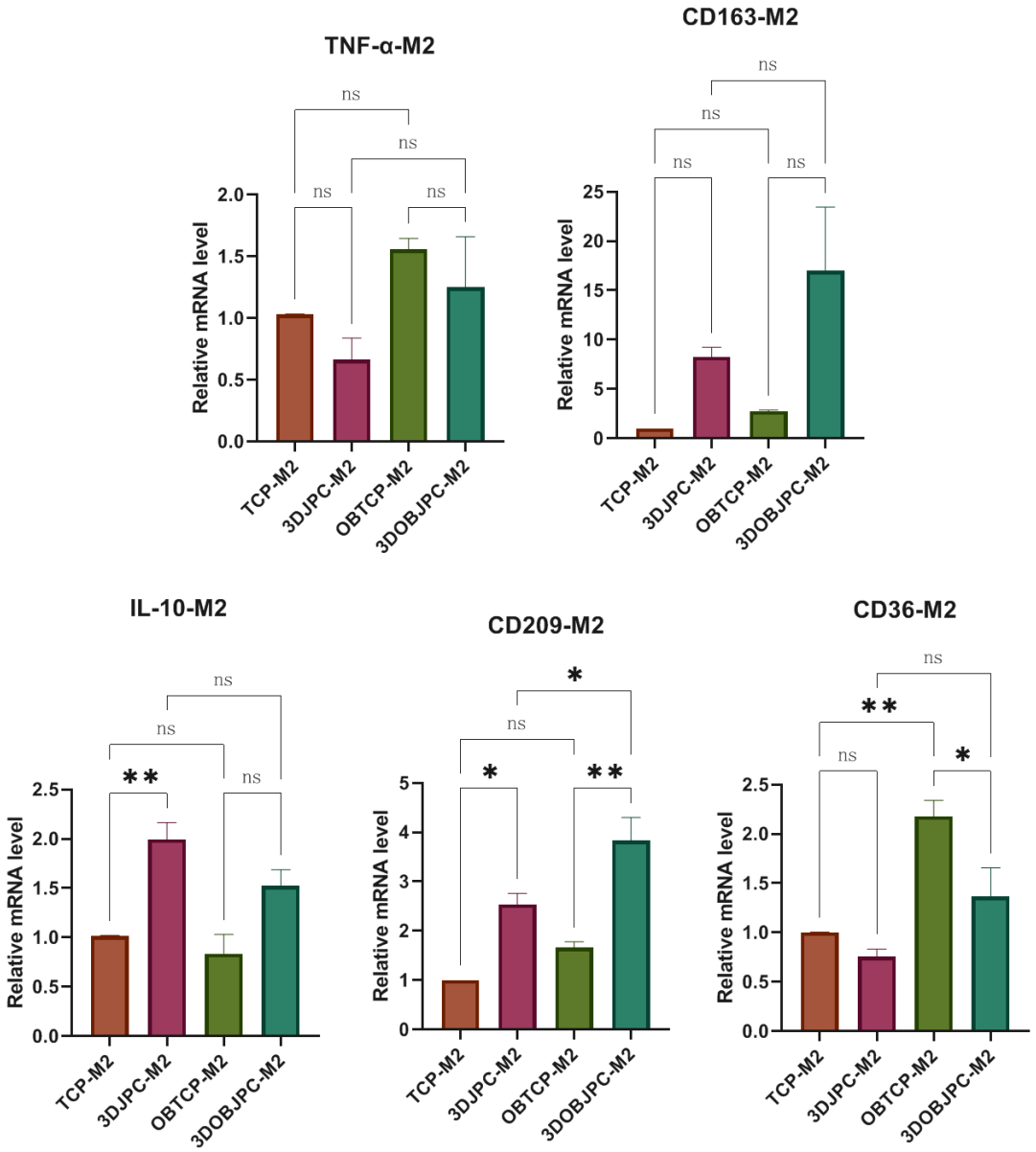

Figure 19. TNF-α, CD163, IL-10, CD209 and CD36 gene expressions of M2 macrophages cocultured with 3DJPCs/3DOBJPCs. Means ± standard error of the mean were calculated and analyzed using one-way analysis of variance (n = 3, * $p < 0.05$, ** $p < 0.01$).

Table 12. Gene expression of M2 macrophages cocultured with 3D-cultured JPCs/OBJPCs.

Genes	TCP-M2	3DJPC-M2	OBTCP-M2	3DOBJPC-M2

TNF-α	1.03 ± 0.00	0.66 ± 0.18	1.56 ± 0.09	1.25 ± 0.41
IL-10	1.01 ± 0.01	1.99 ± 0.17 [a]	0.84 ± 0.20	1.52 ± 0.17
CD163	1.00 ± 0.00	8.26 ± 0.98	2.74 ± 0.12	16.96 ± 6.49
CD209	1.00 ± 0.00	2.54 ± 0.22 [a]	1.66 ± 0.12	3.84 ± 0.46 [b]
CD36	1.00 ± 0.00	0.76 ± 0.08	2.18 ± 0.16	1.37 ± 0.29 [b]

[a] The TCP-M2 and the 3DJPC-M2 groups showed significant differences ($p < 0.05$); [b] The OBTCP-M2 and the 3DOBJPC-M2 groups showed significant differences ($p < 0.05$) (means ± standard error of the mean).

3.4. Analysis of cytokine/chemokine secretion in the horizontal coculture system by proteome profiler arrays (This section published in “He et al., Biomedicines 2021, 9(12), 1753”)

3.4.1. Secretion of M1 macrophages cocultured with 2D-cultured JPCs/OBJPCs

“After five days of horizontal coculture of M1/M2 macrophages and 2D-cultured JPCs/OBJPCs, the chemokine or cytokine production of M1/M2 macrophages was evaluated using proteome profiler arrays. Figure 20 illustrates representative sections of the membranes utilized to demonstrate the distinct dot blot intensities following incubation with the M1 macrophage supernatants. The quantitative analysis of pixel densities indicated significant differences in the chemokine/cytokine secretion of IL-6, CCL2/MCP-1, CXCL1/GRO-α, G-CSF and CCL5/RANTES were found between control groups and coculture groups. Compared with the OBDMEM-M1 group, OBJPC-M1 showed significantly higher expression of IL-6, CCL2/MCP-1, CXCL1/GRO-α and G-CSF. CCL5 showed an obviously decreased expression in the JPC-M1 group when compared with the DMEM-M1 control group. Table 13 provides details about the data.” [72]

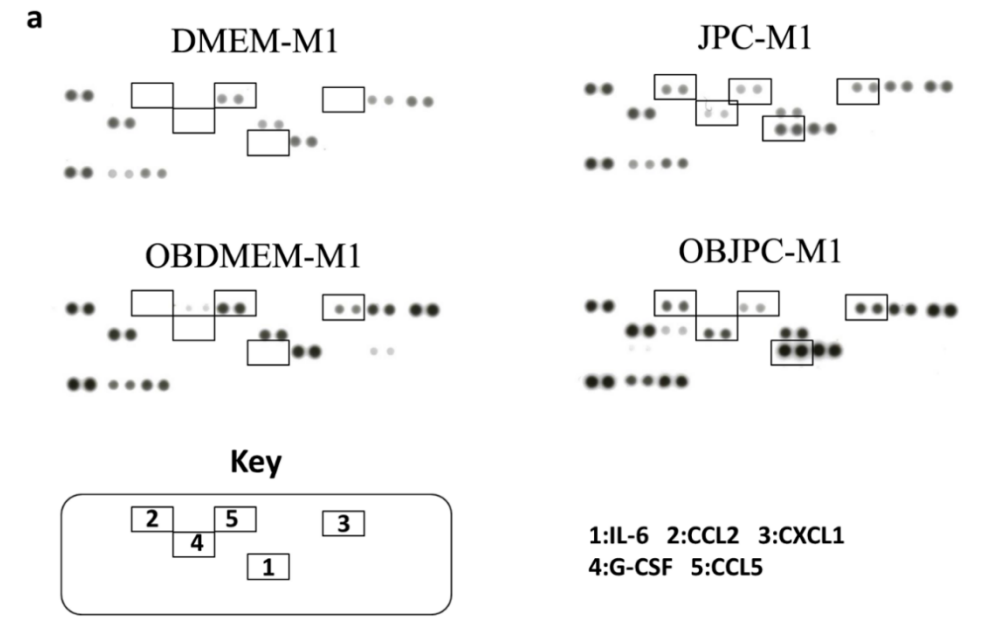
a
DMEM-M1
JPC-M1
OBDMEM-M1
OBJPC-M1
Key
2
5
3
4
1
1:IL-6 2:CCL2 3:CXCL1
4:G-CSF 5:CCL5

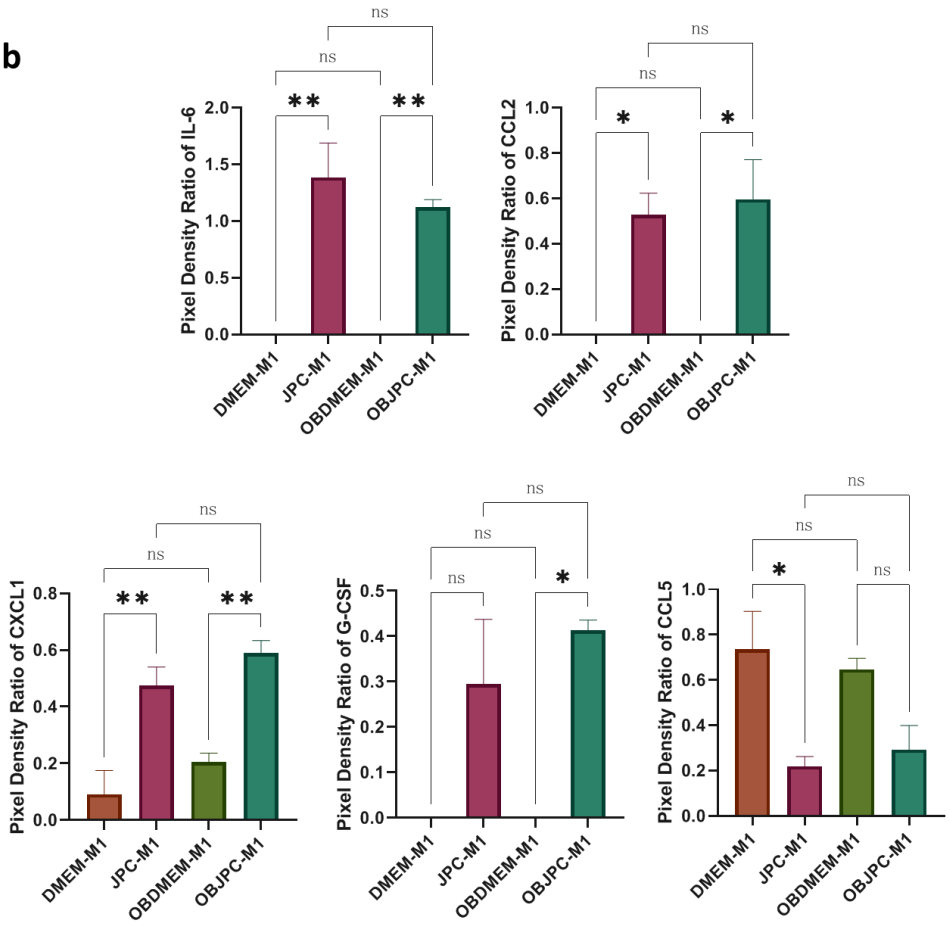
b
Pixel Density Ratio of IL-6
Pixel Density Ratio of CCL2
Pixel Density Ratio of CXCL1
Pixel Density Ratio of G-CSF
Pixel Density Ratio of CCL5
ns
*
**
DMEM-M1
JPC-M1
OBDMEM-M1
OBJPC-M1

Figure 20. Detection of protein expression of supernatants from M1 macrophages cocultured with 2D-cultured JPCs/OBJPCs using proteome profiler arrays. (**a**): After membrane incubation with M1 macrophages supernatants, representative dots of varying intensities were detected (spots in a rectangle: significant differences between the groups). (**b**): Expression of IL-6, CCL2, CXCL1, G-CSF and CCL5 proteins quantified by pixel intensity. Means ± standard error of the mean were calculated and analyzed using one-way analysis of variance (n = 3, * $p < 0.05$, ** $p < 0.01$) [72]. (Images published in "He et al., Biomedicines 2021, 9(12), 1753")

Table 13. The pixel density ratio of proteins in the supernatant from M1 macrophages cocultured with 2D-cultured JPCs/OBJPCs in the horizontal coculture system [72]. (Table published in "He et al., Biomedicines 2021, 9(12), 1753")

Cytokine/Chemokine	DMEM-M1	JPC-M1	OBDMEM-M1	OBJPC-M1
IL-6	0.00 ± 0.00	1.39 ± 0.30 [a]	0.00 ± 0.00	1.12 ± 0.07 [b]
CCL2	0.00 ± 0.00	0.53 ± 0.10 [a]	0.00 ± 0.00	0.60 ± 0.17 [b]
CXCL1	0.09 ± 0.08	0.48 ± 0.06 [a]	0.20 ± 0.03	0.59 ± 0.04 [b]
G-CSF	0.00 ± 0.00	0.29 ± 0.14	0.00 ± 0.00	0.41 ± 0.02 [b]
CCL5	0.74 ± 0.17	0.22 ± 0.04 [a]	0.65 ± 0.05	0.30 ± 0.11

[a] The DMEM-M1 and the JPC-M1 groups showed significant differences ($p < 0.05$); [b] The OBDMEM-M1 and the OBJPC-M1 groups showed significant differences ($p < 0.05$) (means ± standard error of the mean).

3.4.2. Secretion of M2 macrophages cocultured with 2D-cultured JPCs/OBJPCs

"Figure 21 illustrates representative array membranes with dot blots representing the expression of cytokines or chemokines in M2 macrophage supernatants. According to quantitative analysis, IL-6, CCL2 and CXCL12 secretion in the JPC-M2 group were significantly higher compared with those in the DMEM-M2 group. Also, the levels of IL-6, CCL2, CXCL1 and CXCL12 in OBJPC-M2 group were

found to be increased compared with those in the OBDMEM-M2 group. The data are displayed in Table 14.” [72]

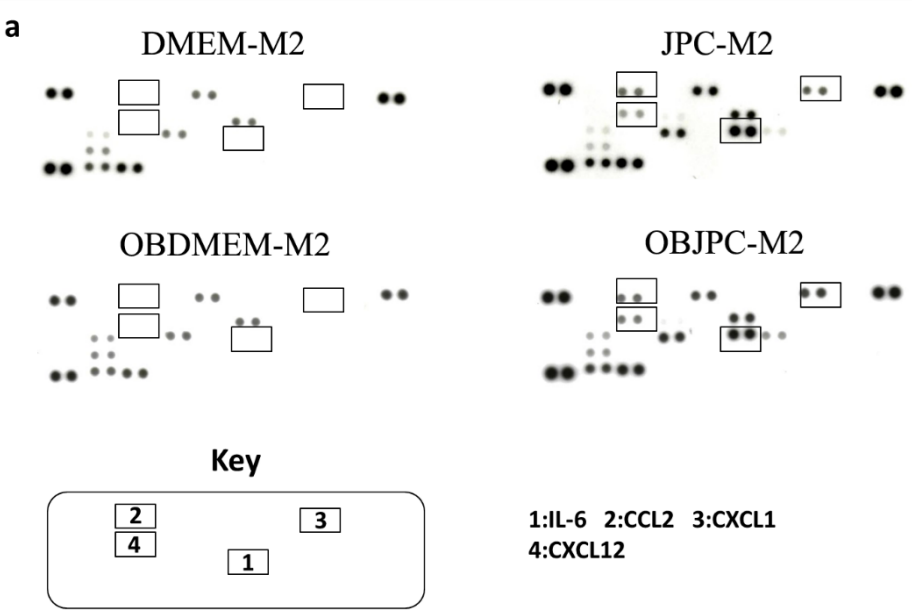

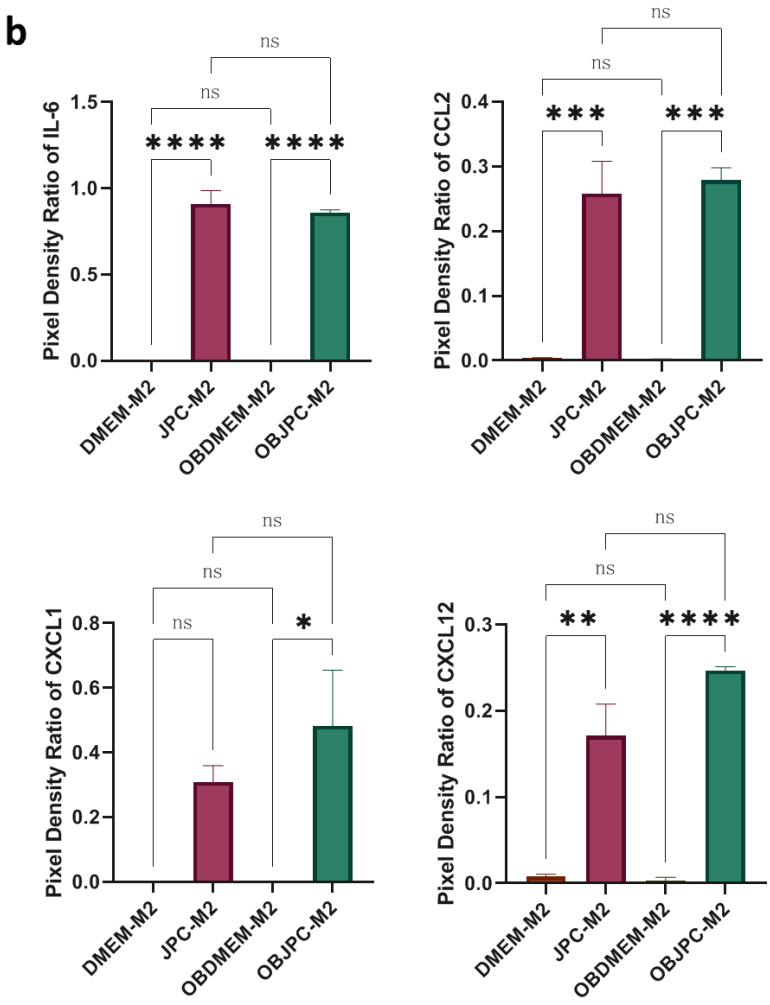

Figure 21. Detection of protein expression of supernatants from M2 macrophages cocultured with 2D-cultured JPCs/OBJPCs using proteome profiler arrays. (**a**): Representative dot blots of varying intensity were measured following membrane treatment with M2 macrophage supernatants (spots in a rectangle: significant differences between the groups). (**b**): Quantification of the pixel intensities associated with the expression of the proteins IL-6, CCL2, CXCL1, and CXCL12. Means ± standard error of the mean were calculated and analyzed using one-way analysis of variance (n = 3, * $p < 0.05$, ** $p < 0.01$, *** $p < 0.001$, **** $p < 0.0001$) [72]. (Images published in “He et al., Biomedicines 2021, 9(12), 1753”)

Table 14. The pixel density ratio of proteins detected in the supernatant from M2 macrophages cocultured with 2D-cultured JPCs/OBJPCs in the horizontal coculture system [72]. (Table published in “He et al., Biomedicines 2021, 9(12),

1753”)

Cytokine/Chemokine	DMEM-M2	JPC-M2	OBDMEM-M2	OBJPC-M2
IL-6	0.00 ± 0.00	0.91 ± 0.08 [a]	0.00 ± 0.00	0.86 ± 0.02 [b]
CCL2	0.00 ± 0.00	0.26 ± 0.05 [a]	0.00 ± 0.00	0.28 ± 0.02 [b]
CXCL1	0.00 ± 0.00	0.31 ± 0.05	0.00 ± 0.00	0.48 ± 0.17 [b]
CXCL12	0.01 ± 0.00	0.17 ± 0.04 [a]	0.00 ± 0.00	0.25 ± 0.00 [b]

[a] The DMEM-M2 and the JPC-M2 groups showed significant differences ($p < 0.05$); [b] The OBDMEM-M2 and the OBJPC-M2 groups showed significant differences ($p < 0.05$) (means ± standard error of the mean).

4. Discussion

4.1. JPCs modulate the macrophage phenotype

In the horizontal coculture system, 2D-cultured JPCs effectively inhibited B7-1 (CD80)/B7-2 (CD86) and CD197 expression of M1 macrophages, suggesting an inhibition of the classical phenotype in M1 macrophages or reduced interactions between M1 macrophages and T lymphocytes [59, 72, 78-80]. On the other side, JPCs under 2D and 3D coculture conditions increased the expression of CD209 and CD163, indicating a transformation of macrophages into the alternative phenotype [72, 81-84]. Besides flow cytometric and gene expression analyses, immunofluorescence staining showed that JPCs were able to decrease CD80 expression on M1 and increase CD209 expression on M2 cells [72]. Therefore, untreated and osteogenically induced 2D- and 3D-cultured JPCs have the capacity to prevent M1 and induce M2 macrophage phenotype polarization in the used horizontal coculture system [72].

A further function of macrophages is the phagocytosis of cell debris and pathogens to maintain inflammatory homeostasis or transformation of osteoclasts through the RANK/RANKL/OPG signalling pathway to perform bone resorption required for bone healing and remodelling [85, 86]. PRRs on the surface of macrophages binding to PAMPs or DAMPs can trigger the activation of phagocytosis [49, 87]. CD36 and CD14, which represent sub-classes of PRRs, expressed on macrophages, can form a complex with Toll-like receptors (TLR) to respond to LPS or lipoteichoic acid (LTA) on gram-negative and gram-positive bacterial cells for further elimination of pathogens [88-90]. 2D-cultured JPCs decreased and increased the expression of scavenger receptors CD36 and PRR CD14 on macrophages, suggesting the modification of pathogens or debris for clearance. Moreover, osteogenically induced 3D-JPCs-constructs decreased the

CD36 gene expression of M2 macrophages, which is coincident with the results from the 2D coculture.

Considering their functional complexity, we summarized the characteristics and essential functions of macrophages markers, which were shown to be regulated by JPCs in our studies, and listed them in Table 15.

Table 15. Characteristics and essential functions of macrophages markers with citations from the literature and detected influence of JPCs in our studies.

Markers	Essential functions	Macrophage phenotype	References	JPCs action
CD80/CD86	binding to T-cell and regulate T cell activation or inhibition	M1	[91]	↓
CD197	binding with CCL19 and CCL21 can trigger an inflammatory reaction	M1	[79, 92]	↓
CD14	detection of bacterial lipopolysaccharide	M1 or M2	[89]	↑
CD36	sensor of microbial diacylated lipoproteins and lipoteichoic acid (through TLR2–TLR6); promoting sterile inflammation (through TLR4–TLR6)	M1 or M2	[88, 93] [94]	↓ in M2
CD209	function of C-type lectin receptor	M2	[81]	↑

CD163	endocytic receptor for haptoglobin–haemoglobin complexes	M2	[95]	↑

4.2. Secretome interactions between JPCs and macrophages

4.2.1. Macrophage secretion

Macrophages orchestrate bone regeneration and play a dynamic regulatory role in bone remodelling. In BTE approaches, the engineered cell-laden scaffold is supposed to be surgically implanted into the bone defect site, accompanied by a cascade of immunological responses in the early stages [96]. The implants and the damaged tissue trigger the release of inflammatory mediators, which effectively recruit inflammatory monocytes to the injury site [97]. Neutrophils, natural killer cells, tissue-resident macrophages and T cells from the damaged tissue release cytokines, such as IFN-γ, to activate the differentiation of the recruited monocytes into an M1-like phenotype of macrophages [49].

In our study, CXCL1, CXCL10, CXCL11 and IL-8 were secreted mainly by M1 macrophages (Table 16) [72]. IL-8 and CXCL1 usually bind to their receptors CXCR1/2 in order to recruit neutrophils [62, 98-100], while the chemokines CXCL9, CXCL10 and CXCL11 play a critical immune chemotactic/recruiting role in the IFN-induced inflammatory response after binding to their receptors CXCR3 (preferentially expressed on immune cells) [62, 101, 102]. These findings suggest that M1 macrophages can release inflammatory chemotactic mediators and are able to recruit different types of immune cells during the onset of inflammation. In addition, IL-8 secretion is also suggested to elicit a proangiogenic effect in the M1 macrophage-mediated inflammatory phase.

M1 macrophages drive inflammation during the initiation phase, while the secreted secretome of M2-type macrophages seems to promote bone remodelling during the later fracture healing stage [85, 103]. It is conceivable that in cell-scaffold-based tissue engineering repair, recruited inflammatory macrophages and bone resident osteal-macrophages promote in early stages inflammation through antigen presentation or paracrine secretion, induce angiogenesis, regulating bone progenitor cell maturation and promoting matrix mineralization [75]. Interleukin-1 receptor antagonist (IL-1RA, an anti-inflammatory cytokine) was abundantly secreted by M2 macrophages in our study [72], which may participate in the anti-inflammatory function of M2 macrophages, usually dominate in the tissue remodelling phase.

Gene expression analyses showed in our study that 3D-cultured untreated and osteogenically induced JPCs could powerfully inhibit the TNF-α gene expression of M1 macrophages. Further, 2D-cultured JPCs/OBJPCs downregulated the gene expression and protein secretion of CCL5 (a factor that can promote M1 macrophages polarization [78]). These results demonstrated effective inhibiting effects of 2D- and 3D-cultured JPCs on the release of inflammatory factors by M1 macrophages. Gene expression of the anti-inflammatory factor IL-10 in M2 macrophage was either in the tendency or obviously upregulated by 2D- or 3D-cultured JPCs, suggesting that JPC-constructs have the potency to mediate the activation of the alternative phenotype of macrophages.

Table 16. The biological functions of detected cytokines/chemokines (ligands) released by JPCs/macrophages [72].

Ligand	Receptor	Secretion	Function to MSCs/immune cells	References

CCL2	CCR2	JPCs	Emigration of monocytes from the bone marrow; Regulating the expression of PDL1 on T cell; Inhibiting TH17 function	[104, 105]
CXCL1	CXCR2	JPCs/M1	Neutrophil recruitment	[62, 106]
CXCL8	CXCR1; CXCR2	JPCs/M1	Neovascularization; Neutrophil recruitment	[107, 108]
CXCL10 CXCL11	CXCR3	JPCs*/M1	Chemoattractants for T cells	[102, 109]
CXCL12	CXCR4	JPCs	MSCs mobilization	[110, 111]
G-CSF	CD114	JPCs*	Neutrophils mobilization	[112]
IL-6	CD126	JPCs	Polarizing monocytes toward IL-10-producing M2	[20, 113]
CCL5	CCR1; CCR3; CCR5	M1	Macrophages recruitment	[114, 115]

*Secretion was activated by LPS/IFN-γ stimulation.

4.2.2. JPCs secretion

MSCs are characterized as self-renewal, show high proliferative capacity, differentiation potential and immunoregulative plasticity, while JPCs show minimum standards of MSCs and possess high osteogenic potential [71-74]. The use of JPCs as a candidate mesenchymal stem cell source for BTE has been investigated in the previous works of our group. These studies demonstrated that JPCs colonialized β-TCP scaffolds could inhibit DC maturation and show good

hemocompatibility [116, 117]. However, the multiple immunosuppressive properties of JPCs/MSCs often depend on the dynamic changes of the inflammatory environment, which may further affect the restoration of immunological homeostasis. TLRs expressed on the surface of MSCs can sense TNF-α/IFN-γ stimulation and polarize into an anti- or- pro-inflammatory phenotype and release distinct immunomodulatory factors [118]. In the work of the present thesis, JPCs were shown to constitutively secrete the chemo- and cytokines CCL2, CXCL1, IL-6 and IL-8 [72]. These factors can regulate monocytic, endothelial and neutrophil functions (Table 16). Furthermore, G-CSF as a neutrophil mobilizer [112] and the chemokines IL8/CXCL10/CXCL11 (CXCR3 ligands) were increasingly released by LPS/IFN-γ stimulated JPCs [72]. These factors may contribute to the recruitment of immune cells as well as to angiogenesis, both functions required in different stages during BTE approaches (Table 16).

In addition, similar to endogenous MSCs, transplanted or infused exogenous MSCs, can migrate to inflamed or injured tissues, mediated by the SDF-1/CXCR4 signalling axis [119, 120]. CXCL12 (SDF-1) is constitutively released by JPCs [72], suggesting that endogenous MSCs might be recruited by JPCs and contribute to further tissue repair during BTE approaches.

In contrast to JPCs, MSCs effects on macrophages are examined in depth. MSC-produced inducible NO synthase (iNOS, in mouse) or indoleamine 2,3-dioxygenase (IDO, in human) induces monocytes to differentiate into IL-10-producing M2 macrophages [121]. M2 macrophages, in turn, inhibit T-cell proliferation in an IL-10-independent manner [121], thereby amplifying the immunosuppressive effects emanated by MSCs [109, 122]. In parallel to the iNOS/IDO axis, MSCs secrete prostaglandin E2 (PGE2) and tumour necrosis factor-inducible gene 6 protein (TSG-6) as further immunosuppressive actors [21].

PGE2 production by MSCs is associated with the induction of the alternative macrophage phenotype [123]. TSG6 produced by MSCs can inhibit immune cells migration to inflamed tissue and induce M2 polarization of macrophages [124-126]. The above-mentioned mode of action of MSCs may provide new ideas for studying the mechanisms of macrophage modification/transition by JPCs.

4.3. Limitations and perspective

In this study, we demonstrated that 2D- and 3D-cultured JPCs could inhibit M1 and promote M2 macrophage polarization within the different coculture systems.

One limitation of the study is the use of the cell line THP-1 and the fact that THP-1-derived macrophages may slightly differ in terms of their expression profile from that of the human peripheral blood-derived macrophages. Whereas Shiratori and co-authors concluded that THP-1 cells are useful for studies analyzing M1 rather than M2 polarization, Tedesco and co-authors concluded in their study that THP-1 cells can be regarded as a simplified model of human macrophages when investigating the polarization mechanism [127, 128].

There are still many challenges in regenerating bone defects with BTE-engineered scaffolds constructed using JPCs. Considering the present study of macrophage regulation by JPCs, the primary limitations are as follows.

Firstly, more functions of lineage differentiation and phagocytosis of macrophages can be further investigated. For example, RANK and RANKL are crucial macro-molecules in the skeleton physiology and regulate macrophages and other immune cells [129, 130]. The elucidation of the RANK/RANKL/OPG signaling pathway regulated by JPCs to induce macrophage differentiation into osteoclasts could be valuable in the context of BTE using JPCs-loaded scaffolds. Furthermore, although some phagocytosis-related cell surface markers, such as scavenger receptor (CD163/CD36) and PRR (CD14), were significantly up- or

down-regulated by JPCs, a deeper analysis of the phagocytic functions to specific pathogens, cell debris, foreign materials or even abnormal cells of cocultured macrophages can be performed in further studies.

In the present study, many chemokines were shown to be secreted by JPCs and macrophages. The chemotactic ability of JPCs for recruiting macrophages, endothelial cells, neutrophils and endogenous MSCs (mediated by the SDF-1/CXCR4 axis) can be further validated with suitable in vitro devices (such as microfluidic systems). These findings can help optimize in vitro generated JPC constructs and predict their biocompatibility for future BTE approaches.

5. Summary

Mesenchymal stem cells (MSCs) can regulate several immune cells and function as sensors or switchers in innate and adaptive immunity. Jaw periosteum-derived mesenchymal stem cells (JPCs) are a promising cell source for bone tissue engineering (BTE) due to their strong osteogenic potential and excellent accessibility. The present study used a direct coculture model and an innovative horizontal coculture system to investigate the phenotypic and underlying paracrine effects of 2D- and 3D-cultured JPCs on macrophage polarization.

In the contact coculture model, JPCs and THP-1 macrophages were directly mixed and cocultured using 24 well plates. For horizontal indirect coculture, the 2D-cultured JPCs were cultivated on conventional plastic material of the coculture plates. The 3D-cultured JPCs were constructed by the cell colonization of β-tricalcium phosphate (β-TCP) scaffolds. Untreated or osteogenically induced 2D/3D-JPCs and THP-1 derived M1/M2 macrophages were cocultured in parallel. After five days of horizontal coculture, M1/M2 macrophages related markers were assessed by flow cytometry or quantitative PCR analysis. In addition, human proteome profiler arrays were used to analyze the cytokines/chemokines secretion in the supernatants of cocultured macrophages.

The cocultured JPCs decreased the CD80 expression of M1 macrophages in the contact coculture model. In the horizontal coculture system, flow cytometry results showed that untreated and osteogenically induced 2D-JPCs reduced CD80, CD86, HLA-DR and CD197 markers expression, while CD14 expression was increased on the surface of M1 macrophages. Osteogenically induced 2D-JPCs decreased CD86 and CD36 expression whereas increased levels of CD209, CD11b and CD14 on the surface of M2 macrophages. PCR results showed a decrease in human RANTES and an increase in CD163 and CD209 mRNA levels in M1 macrophages after the coculture with untreated or osteogenically induced

2D-JPCs. Gene expression levels of TNF-α and CD163 were shown to be respectively decreased and increased by 3D-JPCs in M1 macrophages. M2 macrophages showed a tendency to increase their CD163 gene levels after coculturing with both osteogenically induced 2D- and 3D-JPCs. CD209 mRNA levels in M2 macrophages were obviously increased under the influence of untreated or osteogenically induced 3D-JPCs. In addition, proteome array analyses showed that both JPCs and macrophages secrete various soluble factors under the different coculture conditions, which might be involved in the process of JPC-mediated macrophage polarization.

Therefore, we concluded that 2D- and 3D-cultured JPCs are able to secrete a wide range of factors to convert THP-1 macrophages from the classical M1 towards the alternative M2 phenotype.

6. Zusammenfassung

Mesenchymale Stammzellen (MSC) sind in der Lage, verschiedene Arten von Immunzellen zu regulieren und fungieren als Sensoren oder Schalter in der angeborenen und adaptiven Immunität. Aus dem Kieferperiost gewonnene mesenchymale Stammzellen (JPCs) stellen aufgrund ihres hohen osteogenen Potenzials und ihrer hervorragenden Zugänglichkeit eine vielversprechende Zellquelle für Knochen Tissue Engineering dar. In der vorliegenden Studie wurden ein direktes Ko-Kulturmodell und ein innovatives horizontales Ko-Kultur-System verwendet, um die phänotypischen und die zugrundeliegenden parakrinen Effekte von 2D- und 3D-kultivierten JPCs auf die Makrophagenpolarisierung zu untersuchen.

Im Kontakt-Kokulturmodell wurden JPC und THP-1-Makrophagen direkt gemischt und in 24-Well-Platten kokultiviert. Bei der horizontalen indirekten Kokultur wurden die in 2D kultivierten JPCs auf herkömmlichem Kunststoffmaterial der Kokulturplatten kultiviert. Die 3D-kultivierten JPCs wurden durch die Zellbesiedlung von β-Tricalciumphosphat (β-TCP)-Gerüsten hergestellt. Unbehandelte oder osteogen induzierte 2D/3D-JPCs und THP-1 abgeleitete M1/M2-Makrophagen wurden parallel ko-kultiviert. Nach fünf Tagen horizontaler Ko-Kultur für 2D/3D-gezüchtete JPCs wurden M1/M2-Makrophagen-spezifische Marker mittels Durchflusszytometrie oder quantitativer PCR untersucht. Darüber hinaus wurden die humanen Protein-Profiler-Arrays verwendet, um die Zytokin-/Chemokin-Sekretion aus dem Überstand der Makrophagen in der 2D-Kultur zu analysieren.

Die ko-kultivierten JPCs verringerten die CD80-Expression von M1 Makrophagen im Kontakt-Kokulturmodell. Im horizontalen Kokultursystem zeigten die Ergebnisse der Durchflusszytometrie zeigten, dass unbehandelte und osteogen induzierte 2D-JPCs die Expression der Marker CD80, CD86, HLA-DR und CD197

reduzierten, während die Expression von CD14 auf der Oberfläche von M1-Makrophagen erhöht war. Osteogen induzierte 2D-JPCs verringerten die Expression von CD86 und CD36, während auf der Oberfläche von M2-Makrophagen eine erhöhte Expression von CD209, CD11b und CD14 festgestellt wurden. Die PCR-Ergebnisse zeigten einen Rückgang von humanem RANTES und einen Anstieg der mRNA-Spiegel von CD163 und CD209 in M1-Makrophagen nach der Co-Kultur mit unbehandelten oder osteogen induzierten 2D-JPCs. Der mRNA-Spiegel von TNF-α und CD163 in M1-Makrophagen wurde durch 3D-JPCs ebenfalls verringert bzw. erhöht. M2-Makrophagen zeigten eine Tendenz zu erhöhten CD163-Genspiegeln nach der Ko-Kultur mit osteogen induzierten 2D- und 3D-JPCs. Gleichzeitig wurde der CD209 mRNA-Spiegel in M2-Makrophagen durch unbehandelte oder osteogen induzierte 3D-JPCs deutlich erhöht. Darüber hinaus zeigten Proteom-Array-Analysen, dass sowohl JPCs als auch Makrophagen unter verschiedenen Ko-Kulturbedingungen eine Vielzahl löslicher Faktoren ausschütten, die an der Makrophagenpolarisierung beteiligt sein könnten.

Daraus schlussfolgerten wir, dass 2D- und 3D-kultivierte JPCs in der Lage sind, eine breite Palette von Faktoren zu sezernieren, um THP-1-Makrophagen vom klassischen M1- in den alternativen M2-Phänotyp zu überführen.

7. References

1. Lanza, R.; Langer, R.; Vacanti, J. P.; Atala, A., *Principles of tissue engineering*. Academic press: 2020.
2. Kruyt, M. C.; Dhert, W. J.; Yuan, H.; Wilson, C. E.; van Blitterswijk, C. A.; Verbout, A. J.; de Bruijn, J. D., Bone tissue engineering in a critical size defect compared to ectopic implantations in the goat. *Journal of orthopaedic research : official publication of the Orthopaedic Research Society* **2004,** 22, (3), 544-51.
3. Amini, A. R.; Laurencin, C. T.; Nukavarapu, S. P., Bone tissue engineering: recent advances and challenges. *Critical reviews in biomedical engineering* **2012,** 40, (5), 363-408.
4. Ho-Shui-Ling, A.; Bolander, J.; Rustom, L. E.; Johnson, A. W.; Luyten, F. P.; Picart, C., Bone regeneration strategies: Engineered scaffolds, bioactive molecules and stem cells current stage and future perspectives. *Biomaterials* **2018,** 180, 143-162.
5. Collins, M. N.; Ren, G.; Young, K.; Pina, S.; Reis, R. L.; Oliveira, J. M., Scaffold fabrication technologies and structure/function properties in bone tissue engineering. *Advanced functional materials* **2021,** 31, (21), 2010609.
6. Velasco, M. A.; Narvaez-Tovar, C. A.; Garzon-Alvarado, D. A., Design, materials, and mechanobiology of biodegradable scaffolds for bone tissue engineering. *BioMed research international* **2015,** 2015, 729076.
7. Koons, G. L.; Diba, M.; Mikos, A. G., Materials design for bone-tissue engineering. *Nature Reviews Materials* **2020,** 5, (8), 584-603.
8. Bohner, M.; Santoni, B. L. G.; Dobelin, N., beta-tricalcium phosphate for bone substitution: Synthesis and properties. *Acta biomaterialia* **2020,** 113, 23-41.
9. Meijer, G. J.; de Bruijn, J. D.; Koole, R.; van Blitterswijk, C. A., Cell-based bone tissue engineering. *PLoS medicine* **2007,** 4, (2), e9.

10. Kargozar, S.; Mozafari, M.; Hamzehlou, S.; Brouki Milan, P.; Kim, H.-W.; Baino, F., Bone tissue engineering using human cells: a comprehensive review on recent trends, current prospects, and recommendations. *Applied Sciences* **2019,** 9, (1), 174.
11. Vishwakarma, A.; Sharpe, P.; Songtao, S.; Ramalingam, M., *Stem cell biology and tissue engineering in dental sciences*. Academic Press: 2014.
12. Liu, X.; Li, W.; Fu, X.; Xu, Y., The Immunogenicity and Immune Tolerance of Pluripotent Stem Cell Derivatives. *Frontiers in immunology* **2017,** 8, 645.
13. Knoepfler, P. S., Deconstructing stem cell tumorigenicity: a roadmap to safe regenerative medicine. *Stem cells* **2009,** 27, (5), 1050-6.
14. Caplan, A. I., Mesenchymal stem cells. *Journal of orthopaedic research* **1991,** 9, (5), 641-650.
15. Uccelli, A.; Moretta, L.; Pistoia, V., Mesenchymal stem cells in health and disease. *Nature reviews immunology* **2008,** 8, (9), 726-736.
16. Dominici, M.; Le Blanc, K.; Mueller, I.; Slaper-Cortenbach, I.; Marini, F.; Krause, D.; Deans, R.; Keating, A.; Prockop, D.; Horwitz, E., Minimal criteria for defining multipotent mesenchymal stromal cells. The International Society for Cellular Therapy position statement. *Cytotherapy* **2006,** 8, (4), 315-7.
17. Marolt Presen, D.; Traweger, A.; Gimona, M.; Redl, H., Mesenchymal Stromal Cell-Based Bone Regeneration Therapies: From Cell Transplantation and Tissue Engineering to Therapeutic Secretomes and Extracellular Vesicles. *Frontiers in bioengineering and biotechnology* **2019,** 7, 352.
18. Ankrum, J. A.; Ong, J. F.; Karp, J. M., Mesenchymal stem cells: immune evasive, not immune privileged. *Nature biotechnology* **2014,** 32, (3), 252-60.
19. Shi, Y.; Wang, Y.; Li, Q.; Liu, K.; Hou, J.; Shao, C.; Wang, Y.,

Immunoregulatory mechanisms of mesenchymal stem and stromal cells in inflammatory diseases. *Nature reviews. Nephrology* **2018,** 14, (8), 493-507.

20. Bernardo, M. E.; Fibbe, W. E., Mesenchymal stromal cells: sensors and switchers of inflammation. *Cell stem cell* **2013,** 13, (4), 392-402.
21. Ma, S.; Xie, N.; Li, W.; Yuan, B.; Shi, Y.; Wang, Y., Immunobiology of mesenchymal stem cells. *Cell death and differentiation* **2014,** 21, (2), 216-25.
22. Li, X.; He, X. T.; Kong, D. Q.; Xu, X. Y.; Wu, R. X.; Sun, L. J.; Tian, B. M.; Chen, F. M., M2 Macrophages Enhance the Cementoblastic Differentiation of Periodontal Ligament Stem Cells via the Akt and JNK Pathways. *Stem cells* **2019,** 37, (12), 1567-1580.
23. Loi, F.; Cordova, L. A.; Zhang, R.; Pajarinen, J.; Lin, T. H.; Goodman, S. B.; Yao, Z., The effects of immunomodulation by macrophage subsets on osteogenesis in vitro. *Stem cell research & therapy* **2016,** 7, 15.
24. Zhang, Z. Y.; Teoh, S. H.; Hui, J. H.; Fisk, N. M.; Choolani, M.; Chan, J. K., The potential of human fetal mesenchymal stem cells for off-the-shelf bone tissue engineering application. *Biomaterials* **2012,** 33, (9), 2656-72.
25. Venkataiah, V. S.; Yahata, Y.; Kitagawa, A.; Inagaki, M.; Kakiuchi, Y.; Nakano, M.; Suzuki, S.; Handa, K.; Saito, M., Clinical Applications of Cell-Scaffold Constructs for Bone Regeneration Therapy. *Cells* **2021,** 10, (10), 2687.
26. Macías, I.; Alcorta-Sevillano, N.; Infante, A.; Rodríguez, C. I., Cutting Edge Endogenous Promoting and Exogenous Driven Strategies for Bone Regeneration. *International journal of molecular sciences* **2021,** 22, (14), 7724.
27. Mountziaris, P. M.; Mikos, A. G., Modulation of the inflammatory response for enhanced bone tissue regeneration. *Tissue engineering. Part B,*

Reviews **2008,** 14, (2), 179-86.

28. Li, H.; Shen, S.; Fu, H.; Wang, Z.; Li, X.; Sui, X.; Yuan, M.; Liu, S.; Wang, G.; Guo, Q., Immunomodulatory Functions of Mesenchymal Stem Cells in Tissue Engineering. *Stem cells international* **2019,** 2019, 9671206.
29. Le Blanc, K.; Mougiakakos, D., Multipotent mesenchymal stromal cells and the innate immune system. *Nature reviews. Immunology* **2012,** 12, (5), 383-96.
30. Nishimura, M.; Takase, K.; Suehiro, F.; Murata, H., Candidates cell sources to regenerate alveolar bone from oral tissue. *International journal of dentistry* **2012,** 2012, 857192.
31. Black, J. D.; Tadros, B. J., Bone structure: from cortical to calcium. *Orthopaedics and Trauma* **2020,** 34, (3), 113-119.
32. Watanabe-Takano, H.; Ochi, H.; Chiba, A.; Matsuo, A.; Kanai, Y.; Fukuhara, S.; Ito, N.; Sako, K.; Miyazaki, T.; Tainaka, K.; Harada, I.; Sato, S.; Sawada, Y.; Minamino, N.; Takeda, S.; Ueda, H. R.; Yasoda, A.; Mochizuki, N., Mechanical load regulates bone growth via periosteal Osteocrin. *Cell reports* **2021,** 36, (2), 109380.
33. Moore, E. R.; Zhu, Y. X.; Ryu, H. S.; Jacobs, C. R., Periosteal progenitors contribute to load-induced bone formation in adult mice and require primary cilia to sense mechanical stimulation. *Stem cell research & therapy* **2018,** 9, (1), 190.
34. Feik, S. A.; Storey, E.; Ellender, G., Stress induced periosteal changes. *British journal of experimental pathology* **1987,** 68, (6), 803-13.
35. Hayashi, O.; Katsube, Y.; Hirose, M.; Ohgushi, H.; Ito, H., Comparison of osteogenic ability of rat mesenchymal stem cells from bone marrow, periosteum, and adipose tissue. *Calcified tissue international* **2008,** 82, (3), 238-47.
36. Park, J.-B.; Bae, S.-S.; Lee, P.-W.; Lee, W.; Park, Y.-H.; Kim, H.; Lee, K.;

Kim, I., Comparison of stem cells derived from periosteum and bone marrow of jaw bone and long bone in rabbit models. *Tissue Engineering and Regenerative Medicine* **2012,** 9, (4), 224-230.

37. Groeneveldt, L. C.; Herpelinck, T.; Marechal, M.; Politis, C.; van, I. W. F. J.; Huylebroeck, D.; Geris, L.; Mulugeta, E.; Luyten, F. P., The Bone-Forming Properties of Periosteum-Derived Cells Differ Between Harvest Sites. *Frontiers in cell and developmental biology* **2020,** 8, 554984.
38. Debnath, S.; Yallowitz, A. R.; McCormick, J.; Lalani, S.; Zhang, T.; Xu, R.; Li, N.; Liu, Y.; Yang, Y. S.; Eiseman, M.; Shim, J. H.; Hameed, M.; Healey, J. H.; Bostrom, M. P.; Landau, D. A.; Greenblatt, M. B., Discovery of a periosteal stem cell mediating intramembranous bone formation. *Nature* **2018,** 562, (7725), 133-139.
39. Wanner, Y.; Umrath, F.; Waidmann, M.; Reinert, S.; Alexander, D., Platelet Lysate: The Better Choice for Jaw Periosteal Cell Mineralization. *Stem cells international* **2017,** 2017, 8303959.
40. Brauchle, E.; Carvajal Berrio, D.; Rieger, M.; Schenke-Layland, K.; Reinert, S.; Alexander, D., Raman Spectroscopic Analyses of Jaw Periosteal Cell Mineralization. *Stem cells international* **2017,** 2017, 1651376.
41. Dai, J.; Umrath, F.; Reinert, S.; Alexander, D., Jaw Periosteal Cells Seeded in Beta-Tricalcium Phosphate Inhibit Dendritic Cell Maturation. *Biomolecules* **2020,** 10, (6).
42. Dai, J.; Rottau, D.; Kohler, F.; Reinert, S.; Alexander, D., Effects of Jaw Periosteal Cells on Dendritic Cell Maturation. *Journal of clinical medicine* **2018,** 7, (10).
43. Miyata, R.; van Eeden, S. F., The innate and adaptive immune response induced by alveolar macrophages exposed to ambient particulate matter. *Toxicology and applied pharmacology* **2011,** 257, (2), 209-226.
44. Navegantes, K. C.; de Souza Gomes, R.; Pereira, P. A. T.; Czaikoski, P.

G.; Azevedo, C. H. M.; Monteiro, M. C., Immune modulation of some autoimmune diseases: the critical role of macrophages and neutrophils in the innate and adaptive immunity. *Journal of translational medicine* **2017,** 15, (1), 1-21.

45. Sinder, B. P.; Pettit, A. R.; McCauley, L. K., Macrophages: Their Emerging Roles in Bone. *Journal of bone and mineral research : the official journal of the American Society for Bone and Mineral Research* **2015,** 30, (12), 2140-9.
46. Xia, Z.; Triffitt, J. T., A review on macrophage responses to biomaterials. *Biomedical materials* **2006,** 1, (1), R1.
47. Murray, D.; Rushton, N., Macrophages stimulate bone resorption when they phagocytose particles. *The Journal of bone and joint surgery. British volume* **1990,** 72, (6), 988-992.
48. Epelman, S.; Lavine, K. J.; Randolph, G. J., Origin and functions of tissue macrophages. *Immunity* **2014,** 41, (1), 21-35.
49. Murray, P. J.; Wynn, T. A., Protective and pathogenic functions of macrophage subsets. *Nature reviews. Immunology* **2011,** 11, (11), 723-37.
50. Gerhardt, T.; Ley, K., Monocyte trafficking across the vessel wall. *Cardiovascular research* **2015,** 107, (3), 321-30.
51. van de Laar, L.; Saelens, W.; De Prijck, S.; Martens, L.; Scott, C. L.; Van Isterdael, G.; Hoffmann, E.; Beyaert, R.; Saeys, Y.; Lambrecht, B. N.; Guilliams, M., Yolk Sac Macrophages, Fetal Liver, and Adult Monocytes Can Colonize an Empty Niche and Develop into Functional Tissue-Resident Macrophages. *Immunity* **2016,** 44, (4), 755-68.
52. Aderem, A.; Underhill, D. M., Mechanisms of phagocytosis in macrophages. *Annual review of immunology* **1999,** 17, 593-623.
53. Jakubzick, C. V.; Randolph, G. J.; Henson, P. M., Monocyte differentiation and antigen-presenting functions. *Nature reviews. Immunology* **2017,** 17,

(6), 349-362.

54. Abbas, A. K.; Lichtman, A. H.; Pillai, S., *Cellular and molecular immunology E-book*. Elsevier Health Sciences: 2014.

55. Aderem, A., How to eat something bigger than your head. *Cell* **2002,** 110, (1), 5-8.

56. Korns, D.; Frasch, S. C.; Fernandez-Boyanapalli, R.; Henson, P. M.; Bratton, D. L., Modulation of macrophage efferocytosis in inflammation. *Frontiers in immunology* **2011,** 2, 57.

57. Takeuchi, O.; Akira, S., Pattern recognition receptors and inflammation. *Cell* **2010,** 140, (6), 805-20.

58. Gordon, S., Phagocytosis: An Immunobiologic Process. *Immunity* **2016,** 44, (3), 463-475.

59. Gutcher, I.; Becher, B., APC-derived cytokines and T cell polarization in autoimmune inflammation. *The Journal of clinical investigation* **2007,** 117, (5), 1119-27.

60. Murray, P. J., Macrophage polarization. *Annual review of physiology* **2017,** 79, 541-566.

61. Mills, C. D.; Kincaid, K.; Alt, J. M.; Heilman, M. J.; Hill, A. M., M-1/M-2 macrophages and the Th1/Th2 paradigm. *Journal of immunology* **2000,** 164, (12), 6166-73.

62. Mantovani, A.; Sica, A.; Sozzani, S.; Allavena, P.; Vecchi, A.; Locati, M., The chemokine system in diverse forms of macrophage activation and polarization. *Trends in immunology* **2004,** 25, (12), 677-86.

63. Roszer, T., Understanding the Mysterious M2 Macrophage through Activation Markers and Effector Mechanisms. *Mediators of inflammation* **2015,** 2015, 816460.

64. Lund, M. E.; To, J.; O'Brien, B. A.; Donnelly, S., The choice of phorbol 12-myristate 13-acetate differentiation protocol influences the response of

THP-1 macrophages to a pro-inflammatory stimulus. *Journal of immunological methods* **2016,** 430, 64-70.

65. Daigneault, M.; Preston, J. A.; Marriott, H. M.; Whyte, M. K.; Dockrell, D. H., The identification of markers of macrophage differentiation in PMA-stimulated THP-1 cells and monocyte-derived macrophages. *PloS one* **2010,** 5, (1), e8668.
66. Genin, M.; Clement, F.; Fattaccioli, A.; Raes, M.; Michiels, C., M1 and M2 macrophages derived from THP-1 cells differentially modulate the response of cancer cells to etoposide. *BMC cancer* **2015,** 15, 577.
67. Paschos, N. K.; Brown, W. E.; Eswaramoorthy, R.; Hu, J. C.; Athanasiou, K. A., Advances in tissue engineering through stem cell-based co-culture. *Journal of tissue engineering and regenerative medicine* **2015,** 9, (5), 488-503.
68. Bogdanowicz, D. R.; Lu, H. H., Studying cell-cell communication in co-culture. *Biotechnology journal* **2013,** 8, (4), 395-6.
69. Shimasaki, T.; Yamamoto, S.; Arisawa, T., Exosome Research and Co-culture Study. *Biological & pharmaceutical bulletin* **2018,** 41, (9), 1311-1321.
70. Vis, M. A. M.; Ito, K.; Hofmann, S., Impact of Culture Medium on Cellular Interactions in in vitro Co-culture Systems. *Frontiers in bioengineering and biotechnology* **2020,** 8, 911.
71. He, F.; Umrath, F.; Reinert, S.; Alexander, D., Jaw Periosteum-Derived Mesenchymal Stem Cells Regulate THP-1-Derived Macrophage Polarization. *International journal of molecular sciences* **2021,** 22, (9).
72. He, F.; Umrath, F.; von Ohle, C.; Reinert, S.; Alexander, D., Analysis of the Influence of Jaw Periosteal Cells on Macrophages Phenotype Using an Innovative Horizontal Coculture System. *Biomedicines* **2021,** 9, (12), 1753.
73. Umrath, F.; Weber, M.; Reinert, S.; Wendel, H. P.; Avci-Adali, M.; Alexander,

D., iPSC-Derived MSCs Versus Originating Jaw Periosteal Cells: Comparison of Resulting Phenotype and Stem Cell Potential. *International journal of molecular sciences* **2020,** 21, (2).

74. Brauchle, E.; Carvajal Berrio, D.; Rieger, M.; Schenke-Layland, K.; Reinert, S.; Alexander, D., Raman spectroscopic analyses of jaw periosteal cell mineralization. *Stem cells international* **2017,** 2017.

75. Niu, Y.; Wang, Z.; Shi, Y.; Dong, L.; Wang, C., Modulating macrophage activities to promote endogenous bone regeneration: Biological mechanisms and engineering approaches. *Bioactive materials* **2021,** 6, (1), 244-261.

76. Dai, J.; Rottau, D.; Kohler, F.; Reinert, S.; Alexander, D., Effects of jaw periosteal cells on dendritic cell maturation. *Journal of clinical medicine* **2018,** 7, (10), 312.

77. McKee, C.; Chaudhry, G. R., Advances and challenges in stem cell culture. *Colloids and surfaces. B, Biointerfaces* **2017,** 159, 62-77.

78. Li, M.; Sun, X.; Zhao, J.; Xia, L.; Li, J.; Xu, M.; Wang, B.; Guo, H.; Yu, C.; Gao, Y.; Wu, H.; Kong, X.; Xia, Q., CCL5 deficiency promotes liver repair by improving inflammation resolution and liver regeneration through M2 macrophage polarization. *Cellular & molecular immunology* **2020,** 17, (7), 753-764.

79. Tateyama, M.; Fujihara, K.; Misu, T.; Itoyama, Y., CCR7+ myeloid dendritic cells together with CCR7+ T cells and CCR7+ macrophages invade CCL19+ nonnecrotic muscle fibers in inclusion body myositis. *Journal of the neurological sciences* **2009,** 279, (1-2), 47-52.

80. Sharpe, A. H.; Freeman, G. J., The B7-CD28 superfamily. *Nature reviews. Immunology* **2002,** 2, (2), 116-26.

81. McGreal, E. P.; Miller, J. L.; Gordon, S., Ligand recognition by antigen-presenting cell C-type lectin receptors. *Current opinion in immunology*

2005, 17, (1), 18-24.

82. Yao, Y.; Xu, X. H.; Jin, L., Macrophage Polarization in Physiological and Pathological Pregnancy. *Frontiers in immunology* **2019,** 10, 792.
83. Landis, R. C.; Philippidis, P.; Domin, J.; Boyle, J. J.; Haskard, D. O., Haptoglobin Genotype-Dependent Anti-Inflammatory Signaling in CD163(+) Macrophages. *International journal of inflammation* **2013,** 2013, 980327.
84. Fabriek, B. O.; van Bruggen, R.; Deng, D. M.; Ligtenberg, A. J.; Nazmi, K.; Schornagel, K.; Vloet, R. P.; Dijkstra, C. D.; van den Berg, T. K., The macrophage scavenger receptor CD163 functions as an innate immune sensor for bacteria. *Blood* **2009,** 113, (4), 887-892.
85. Pajarinen, J.; Lin, T.; Gibon, E.; Kohno, Y.; Maruyama, M.; Nathan, K.; Lu, L.; Yao, Z.; Goodman, S. B., Mesenchymal stem cell-macrophage crosstalk and bone healing. *Biomaterials* **2019,** 196, 80-89.
86. Boyce, B. F.; Xing, L., Functions of RANKL/RANK/OPG in bone modeling and remodeling. *Archives of biochemistry and biophysics* **2008,** 473, (2), 139-46.
87. Amarante-Mendes, G. P.; Adjemian, S.; Branco, L. M.; Zanetti, L. C.; Weinlich, R.; Bortoluci, K. R., Pattern Recognition Receptors and the Host Cell Death Molecular Machinery. *Frontiers in immunology* **2018,** 9, 2379.
88. Triantafilou, M.; Gamper, F. G.; Haston, R. M.; Mouratis, M. A.; Morath, S.; Hartung, T.; Triantafilou, K., Membrane sorting of toll-like receptor (TLR)-2/6 and TLR2/1 heterodimers at the cell surface determines heterotypic associations with CD36 and intracellular targeting. *The Journal of biological chemistry* **2006,** 281, (41), 31002-11.
89. Kitchens, R. L., Role of CD14 in cellular recognition of bacterial lipopolysaccharides. *Chemical immunology* **2000,** 74, 61-82.
90. Ranoa, D. R. E.; Kelley, S. L.; Tapping, R. I., Human lipopolysaccharide-

binding protein (LBP) and CD14 independently deliver triacylated lipoproteins to Toll-like receptor 1 (TLR1) and TLR2 and enhance formation of the ternary signaling complex. *The Journal of biological chemistry* **2013,** 288, (14), 9729-9741.

91. Lanier, L. L.; O'Fallon, S.; Somoza, C.; Phillips, J. H.; Linsley, P. S.; Okumura, K.; Ito, D.; Azuma, M., CD80 (B7) and CD86 (B70) provide similar costimulatory signals for T cell proliferation, cytokine production, and generation of CTL. *Journal of immunology* **1995,** 154, (1), 97-105.
92. Kwiecien, I.; Polubiec-Kownacka, M.; Dziedzic, D.; Wolosz, D.; Rzepecki, P.; Domagala-Kulawik, J., CD163 and CCR7 as markers for macrophage polarization in lung cancer microenvironment. *Central-European journal of immunology* **2019,** 44, (4), 395-402.
93. Hoebe, K.; Georgel, P.; Rutschmann, S.; Du, X.; Mudd, S.; Crozat, K.; Sovath, S.; Shamel, L.; Hartung, T.; Zahringer, U.; Beutler, B., CD36 is a sensor of diacylglycerides. *Nature* **2005,** 433, (7025), 523-7.
94. Stewart, C. R.; Stuart, L. M.; Wilkinson, K.; van Gils, J. M.; Deng, J.; Halle, A.; Rayner, K. J.; Boyer, L.; Zhong, R.; Frazier, W. A.; Lacy-Hulbert, A.; El Khoury, J.; Golenbock, D. T.; Moore, K. J., CD36 ligands promote sterile inflammation through assembly of a Toll-like receptor 4 and 6 heterodimer. *Nature immunology* **2010,** 11, (2), 155-61.
95. Kristiansen, M.; Graversen, J. H.; Jacobsen, C.; Sonne, O.; Hoffman, H. J.; Law, S. K.; Moestrup, S. K., Identification of the haemoglobin scavenger receptor. *Nature* **2001,** 409, (6817), 198-201.
96. Crupi, A.; Costa, A.; Tarnok, A.; Melzer, S.; Teodori, L., Inflammation in tissue engineering: The Janus between engraftment and rejection. *European journal of immunology* **2015,** 45, (12), 3222-36.
97. Saleh, L. S.; Bryant, S. J., The Host Response in Tissue Engineering: Crosstalk Between Immune cells and Cell-laden Scaffolds. *Current*

opinion in biomedical engineering **2018,** 6, 58-65.

98. Martin, C.; Burdon, P. C.; Bridger, G.; Gutierrez-Ramos, J. C.; Williams, T. J.; Rankin, S. M., Chemokines acting via CXCR2 and CXCR4 control the release of neutrophils from the bone marrow and their return following senescence. *Immunity* **2003,** 19, (4), 583-93.
99. Eash, K. J.; Greenbaum, A. M.; Gopalan, P. K.; Link, D. C., CXCR2 and CXCR4 antagonistically regulate neutrophil trafficking from murine bone marrow. *The Journal of clinical investigation* **2010,** 120, (7), 2423-31.
100. Murphy, P. M.; Baggiolini, M.; Charo, I. F.; Hebert, C. A.; Horuk, R.; Matsushima, K.; Miller, L. H.; Oppenheim, J. J.; Power, C. A., International union of pharmacology. XXII. Nomenclature for chemokine receptors. *Pharmacological reviews* **2000,** 52, (1), 145-76.
101. Kuo, P. T.; Zeng, Z.; Salim, N.; Mattarollo, S.; Wells, J. W.; Leggatt, G. R., The Role of CXCR3 and Its Chemokine Ligands in Skin Disease and Cancer. *Frontiers in medicine* **2018,** 5, 271.
102. Tokunaga, R.; Zhang, W.; Naseem, M.; Puccini, A.; Berger, M. D.; Soni, S.; McSkane, M.; Baba, H.; Lenz, H. J., CXCL9, CXCL10, CXCL11/CXCR3 axis for immune activation - A target for novel cancer therapy. *Cancer treatment reviews* **2018,** 63, 40-47.
103. Soehnlein, O.; Lindbom, L., Phagocyte partnership during the onset and resolution of inflammation. *Nature reviews. Immunology* **2010,** 10, (6), 427-39.
104. Tsou, C. L.; Peters, W.; Si, Y.; Slaymaker, S.; Aslanian, A. M.; Weisberg, S. P.; Mack, M.; Charo, I. F., Critical roles for CCR2 and MCP-3 in monocyte mobilization from bone marrow and recruitment to inflammatory sites. *The Journal of clinical investigation* **2007,** 117, (4), 902-9.
105. Rafei, M.; Campeau, P. M.; Aguilar-Mahecha, A.; Buchanan, M.; Williams, P.; Birman, E.; Yuan, S.; Young, Y. K.; Boivin, M. N.; Forner, K.; Basik, M.;

Galipeau, J., Mesenchymal stromal cells ameliorate experimental autoimmune encephalomyelitis by inhibiting CD4 Th17 T cells in a CC chemokine ligand 2-dependent manner. *Journal of immunology* **2009,** 182, (10), 5994-6002.

106. Sawant, K. V.; Poluri, K. M.; Dutta, A. K.; Sepuru, K. M.; Troshkina, A.; Garofalo, R. P.; Rajarathnam, K., Chemokine CXCL1 mediated neutrophil recruitment: Role of glycosaminoglycan interactions. *Scientific reports* **2016,** 6, 33123.
107. Kim, S. W.; Zhang, H. Z.; Guo, L.; Kim, J. M.; Kim, M. H., Amniotic mesenchymal stem cells enhance wound healing in diabetic NOD/SCID mice through high angiogenic and engraftment capabilities. *PloS one* **2012,** 7, (7), e41105.
108. de Oliveira, S.; Reyes-Aldasoro, C. C.; Candel, S.; Renshaw, S. A.; Mulero, V.; Calado, A., Cxcl8 (IL-8) mediates neutrophil recruitment and behavior in the zebrafish inflammatory response. *Journal of immunology* **2013,** 190, (8), 4349-59.
109. Ren, G.; Zhang, L.; Zhao, X.; Xu, G.; Zhang, Y.; Roberts, A. I.; Zhao, R. C.; Shi, Y., Mesenchymal stem cell-mediated immunosuppression occurs via concerted action of chemokines and nitric oxide. *Cell stem cell* **2008,** 2, (2), 141-50.
110. Hu, C.; Yong, X.; Li, C.; Lu, M.; Liu, D.; Chen, L.; Hu, J.; Teng, M.; Zhang, D.; Fan, Y.; Liang, G., CXCL12/CXCR4 axis promotes mesenchymal stem cell mobilization to burn wounds and contributes to wound repair. *The Journal of surgical research* **2013,** 183, (1), 427-34.
111. Liu, X.; Duan, B.; Cheng, Z.; Jia, X.; Mao, L.; Fu, H.; Che, Y.; Ou, L.; Liu, L.; Kong, D., SDF-1/CXCR4 axis modulates bone marrow mesenchymal stem cell apoptosis, migration and cytokine secretion. *Protein Cell* **2011,** 2, (10), 845-54.

112. Semerad, C. L.; Liu, F.; Gregory, A. D.; Stumpf, K.; Link, D. C., G-CSF is an essential regulator of neutrophil trafficking from the bone marrow to the blood. *Immunity* **2002,** 17, (4), 413-23.

113. Eggenhofer, E.; Hoogduijn, M. J., Mesenchymal stem cell-educated macrophages. *Transplantation research* **2012,** 1, (1), 12.

114. Keophiphath, M.; Rouault, C.; Divoux, A.; Clement, K.; Lacasa, D., CCL5 promotes macrophage recruitment and survival in human adipose tissue. *Arteriosclerosis, thrombosis, and vascular biology* **2010,** 30, (1), 39-45.

115. Lee, C. M.; Peng, H. H.; Yang, P.; Liou, J. T.; Liao, C. C.; Day, Y. J., C-C Chemokine Ligand-5 is critical for facilitating macrophage infiltration in the early phase of liver ischemia/reperfusion injury. *Scientific reports* **2017,** 7, (1), 3698.

116. Weber, M.; Umrath, F.; Steinle, H.; Schmitt, L. F.; Yu, L. T.; Schlensak, C.; Wendel, H. P.; Reinert, S.; Alexander, D.; Avci-Adali, M., Influence of Human Jaw Periosteal Cells Seeded beta-Tricalcium Phosphate Scaffolds on Blood Coagulation. *International journal of molecular sciences* **2021,** 22, (18).

117. Dai, J.; Umrath, F.; Reinert, S.; Alexander, D., Jaw Periosteal Cells Seeded in Beta-Tricalcium Phosphate Inhibit Dendritic Cell Maturation. *Biomolecules* **2020,** 10, (6), 887.

118. Nemeth, K.; Mayer, B.; Mezey, E., Modulation of bone marrow stromal cell functions in infectious diseases by toll-like receptor ligands. *Journal of molecular medicine* **2010,** 88, (1), 5-10.

119. Park, D.; Spencer, J. A.; Koh, B. I.; Kobayashi, T.; Fujisaki, J.; Clemens, T. L.; Lin, C. P.; Kronenberg, H. M.; Scadden, D. T., Endogenous bone marrow MSCs are dynamic, fate-restricted participants in bone maintenance and regeneration. *Cell stem cell* **2012,** 10, (3), 259-72.

120. Li, J.; Guo, W.; Xiong, M.; Han, H.; Chen, J.; Mao, D.; Tang, B.; Yu, H.;

Zeng, Y., Effect of SDF-1/CXCR4 axis on the migration of transplanted bone mesenchymal stem cells mobilized by erythropoietin toward lesion sites following spinal cord injury. *International journal of molecular medicine* **2015,** 36, (5), 1205-14.

121. Francois, M.; Romieu-Mourez, R.; Li, M.; Galipeau, J., Human MSC suppression correlates with cytokine induction of indoleamine 2,3-dioxygenase and bystander M2 macrophage differentiation. *Molecular therapy : the journal of the American Society of Gene Therapy* **2012,** 20, (1), 187-95.
122. Su, J.; Chen, X.; Huang, Y.; Li, W.; Li, J.; Cao, K.; Cao, G.; Zhang, L.; Li, F.; Roberts, A. I.; Kang, H.; Yu, P.; Ren, G.; Ji, W.; Wang, Y.; Shi, Y., Phylogenetic distinction of iNOS and IDO function in mesenchymal stem cell-mediated immunosuppression in mammalian species. *Cell death and differentiation* **2014,** 21, (3), 388-96.
123. Vasandan, A. B.; Jahnavi, S.; Shashank, C.; Prasad, P.; Kumar, A.; Prasanna, S. J., Human Mesenchymal stem cells program macrophage plasticity by altering their metabolic status via a PGE2-dependent mechanism. *Scientific reports* **2016,** 6, 38308.
124. Dyer, D. P.; Salanga, C. L.; Johns, S. C.; Valdambrini, E.; Fuster, M. M.; Milner, C. M.; Day, A. J.; Handel, T. M., The Anti-inflammatory Protein TSG-6 Regulates Chemokine Function by Inhibiting Chemokine/Glycosaminoglycan Interactions. *The Journal of biological chemistry* **2016,** 291, (24), 12627-12640.
125. Song, W. J.; Li, Q.; Ryu, M. O.; Ahn, J. O.; Ha Bhang, D.; Chan Jung, Y.; Youn, H. Y., TSG-6 Secreted by Human Adipose Tissue-derived Mesenchymal Stem Cells Ameliorates DSS-induced colitis by Inducing M2 Macrophage Polarization in Mice. *Scientific reports* **2017,** 7, (1), 5187.
126. Mittal, M.; Tiruppathi, C.; Nepal, S.; Zhao, Y. Y.; Grzych, D.; Soni, D.;

Prockop, D. J.; Malik, A. B., TNFalpha-stimulated gene-6 (TSG6) activates macrophage phenotype transition to prevent inflammatory lung injury. *Proceedings of the National Academy of Sciences of the United States of America* **2016,** 113, (50), E8151-E8158.

127. Shiratori, H.; Feinweber, C.; Luckhardt, S.; Linke, B.; Resch, E.; Geisslinger, G.; Weigert, A.; Parnham, M. J., THP-1 and human peripheral blood mononuclear cell-derived macrophages differ in their capacity to polarize in vitro. *Molecular immunology* **2017,** 88, 58-68.
128. Tedesco, S.; De Majo, F.; Kim, J.; Trenti, A.; Trevisi, L.; Fadini, G. P.; Bolego, C.; Zandstra, P. W.; Cignarella, A.; Vitiello, L., Convenience versus Biological Significance: Are PMA-Differentiated THP-1 Cells a Reliable Substitute for Blood-Derived Macrophages When Studying in Vitro Polarization? *Frontiers in pharmacology* **2018,** 9, 71.
129. Rao, S.; Cronin, S. J. F.; Sigl, V.; Penninger, J. M., RANKL and RANK: From Mammalian Physiology to Cancer Treatment. *Trends in cell biology* **2018,** 28, (3), 213-223.
130. Huang, R.; Wang, X.; Zhou, Y.; Xiao, Y., RANKL-induced M1 macrophages are involved in bone formation. *Bone research* **2017,** 5, 17019.

Declaration of Contribution

This study was conducted in the Research Laboratory of the Department of Oral and Maxillofacial Surgery, University Hospital Tübingen, under the supervision of Prof. Dorothea Alexander.

Professor Dorothea Alexander-Friedrich contributed to the research's concepts and hypotheses and designed the experiments. The experimental methods were selected by Prof. Dorothea Alexander-Friedrich, myself and Dr. Felix Umrath. The original manuscript was written by myself and corrected/reviewed by Prof. Dorothea Alexander-Friedrich. Prof. Siegmar Reinert contributed to patient recruitment during the experiment performance. The resources during this experimental performance were supported by Prof. Dorothea Alexander-Friedrich, Prof. Siegmar Reinert. and Prof. Christiane von Ohle.

Parts of my thesis have been published in “Fang He, Felix Umrath, Christiane von Ohle, Siegmar Reinert, Dorothea Alexander. Analysis of the Influence of Jaw Periosteal Cells on Macrophages Phenotype Using an Innovative Horizontal Coculture System[J]. Biomedicines, 2021, 9(12): 1753.” and “Fang He, Felix Umrath, Siegmar Reinert, Dorothea Alexander. Jaw Periosteum-Derived Mesenchymal Stem Cells Regulate THP-1-Derived Macrophage Polarization[J]. International journal of molecular sciences, 2021, 22(9): 4310.”.

For my thesis, I conducted all experiments and analyzed the data by myself. I therefore certify that the thesis is my own work.

Acknowledgement

I would like to offer my heartfelt appreciation to the following individuals and organizations:

First, many sincerely grateful appreciation to my supervisors, Prof. Dorothea Alexander-Friedrich and Prof. Siegmar Reinert, for taking care of me during my studies in Germany and for their intellectual mentoring and project costs acquisition for the experiments required for my project. With their assistance, I was able to increase my knowledge and broaden my horizon.

Furthermore, I would like to thank Dr. Felix Umrath, Prof. Christiane von Ohle, and Inka Schumacher who provided me with support for experimental methods. I want to offer my most profound appreciation to my dear colleagues and friends. I appreciate the time we have shared.

I want to acknowledge the assistance of the Deutsche Forschungsgemeinschaft and the University of Tübingen's Open Access Publishing Fund.

The China Scholarship Council (CSC) is gratefully acknowledged for the financial support of me (No. 201908080135).

Finally, I want to express my gratitude to my family, particularly my parents, for their encouragement and support during my studies.